Schweizerische Eidgenossenschaft
Confédération suisse
Confederazione Svizzera
Confederaziun svizra

Federal Department of the Environment, Transport, Energy and Communications DETEC

Swiss Federal Office of Energy SFOE
Energy Research and Cleantech

Final report dated 31.06.2023

SmartHiFe^2

A novel iron-based catalytic biogas upgrade concept

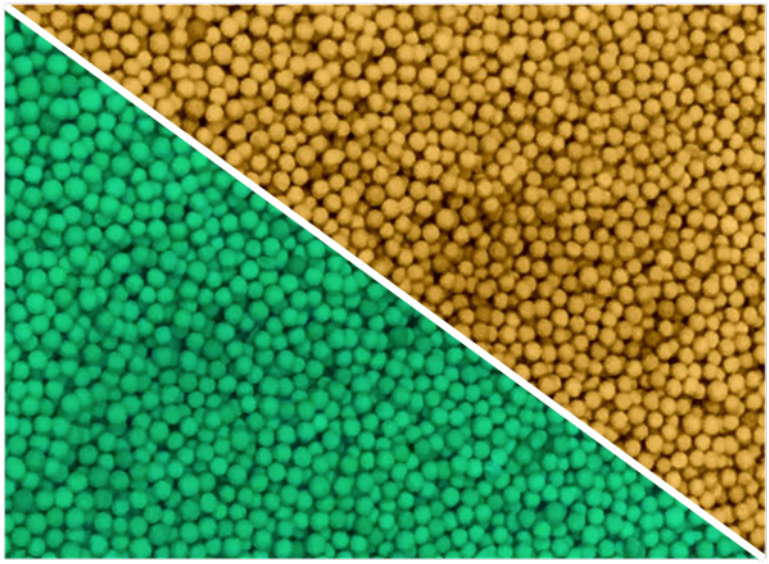

Source: ©Heel 2020

Date: 31.06.2023

Location: Bern

Publisher:
Swiss Federal Office of Energy SFOE
Energy Research and Cleantech
CH-3003 Bern
www.bfe.admin.ch

Subsidy recipients:
OST
UMTEC
Oberseestrasse 10,
8640 Rapperswil-Jona

www.umtec.ch

Authors:
Andre Heel, OST, andre.heel@ost.ch
Bastian Welte, OST, bastian.welte@ost.ch
Stefanie Mizuno, OST, stefanie.mizuno@ost.ch

SFOE project coordinators:
SFOE head of domain: Sandra Hermle, sandra.hermle@bfe.admin.ch
SFOE programme manager: Sandra Hermle, sandra.hermle@bfe.admin.ch

SFOE contract number: SI/502053-01

Zusammenfassung

Das Hauptziel dieses Projekts ist die Entwicklung einer hocheffizienten Sorptions-Methanisierungstechnologie für eine Biogasaufbereitung im Hinblick auf die Bewältigung der noch bestehenden Hindernisse für die Industrialisierung. Diese Hindernisse sind die unzureichende Wirtschaftlichkeit des Ni-Katalysators, dessen Schwefelempfindlichkeit und die Einbindung in einen skalierbaren industriellen Prozess. Die wissenschaftliche Durchdringung ist daher auf ein technologisch-wirtschaftlich zuverlässiges System mit geringerer Umweltbelastung und dessen Integration im Biogasbereich ausgerichtet. In der Förderperiode wurde ein zusätzlicher Weg zur Herstellung von Fe-funktionalisierten Katalysator Pellets etabliert. Dieser wurde speziell für die Verwendung Pulverförmiger Edukte ausgelegt. Es konnten auf diese Weise grössere Mengen an Katalysatorpellets (>200 g) hergestellt, in der eigenen Hochdruckapparatur integriert und in der CO_2 Methanisierungen erprobt werden. Dabei wurde ein deutlicher Sorptionseffekt auf die Reaktion gemessen. Dieser ist für das vorliegende Fe-basierte System neben Druck und Temperatur auch von Faktoren wie der eingesetzten Fe-Vorläuferverbindung abhängig. Monometallische Fe-Katalysatoren schienen anfällig für einen Phasenwechsel während der Methanisierung zu sein. XRD-Messungen zeigten die Bildung einer irreversiblen Eisenkarbidphase. Die Dotierung mit geringen Mengen an Kobalt führte zu einer besseren Leistung mit einer maximalen CO_2-Umwandlung von ~100% bei einer CH_4-Selektivität von bis zu 97%. Darüber hinaus wurden erste Untersuchungen zur Degradierung der Materialien durchgeführt. Das Co-dotierte Material zeigte sich über 10 Reaktionszyklen eine stabile Performance. Mittels TGA konnte gezeigt werden, dass es nicht zur Kohlenstoffanreicherung an den katalytischen Zentren kommt. Die Errungenschaften dieses Projekts haben die Reife der sorptionsgestützten Methanisierungstechnologie, die nun im quasikontinuierlichen Modus betrieben werden kann, erhöht, und es wurden kosteneffizientere katalytische Materialien mit geringeren Auswirkungen auf die Umwelt entwickelt.

Sommario

L'obiettivo principale di questo progetto è lo sviluppo di una tecnologia di metanazione altamente efficiente potenziata mediante adsorbimento per la purificazione del biogas. Si vogliono così affrontare i rimanenti ostacoli verso l'industrializzazione di questa tecnologia. Tali ostacoli riguardano il costo del catalizzatore attivo al nichel e la sua sensibilità al solfuro. L'ulteriore sviluppo scientifico è quindi orientato verso un sistema tecnologicamente ed economicamente affidabile e la sua scalabilità. Durante il progetto, è stata individuata una via aggiuntiva per la produzione di pellet di catalizzatore funzionalizzato al ferro. In questo modo, sono state prodotte grandi quantità di pellet di catalizzatore (> 200 g), installate nell'apparato ad alta pressione in sede e testate per la metanazione del CO_2. È stato misurato un effetto di potenziamento dell'adsorbimento. Per il sistema a base di ferro in questione, il potenziamento dipende non solo dalla pressione e dalla temperatura, ma anche da fattori come il precursore di ferro utilizzato nella preparazione del materiale. I catalizzatori monometallici a base di ferro sembravano inclini a un cambiamento di fase durante la metanazione, e una fase persistente di carburo di ferro è stata identificata mediante Diffrazione dei raggi X (XRD). L'aggiunta di cobalto ha portato a una migliore performance con una conversione massima di ~ 100% e una selettività di CH4 fino al 97%. Inoltre, sono state condotte le prime indagini sulla degradazione dei materiali. Il materiale con aggiunta di cobalto ha presentato una performance stabile in fino a dieci cicli di reazione senza accumulo di carbonio, come indicato dai risultati della analisi termogravimetrica. I risultati ottenuti in questo progetto hanno aumentato la maturità della tecnologia di metanazione potenziata mediante adsorbimento, che ora può essere utilizzata in modalità quasi-continua con materiali catalitici a base di metalli non nobili con un impatto ambientale ridotto.

Summary

The main goal of this project is the development of a highly efficient sorption-enhanced methanation technology for a biogas upgrade concerning tackling the remaining obstacles towards industrialization. Said obstacles are the cost of the catalytic active Ni metal and its sulfur sensitivity. Scientific penetration is therefore aligned towards a technologically and economically, reliable system and its upscaling. During the funding period, an additional route to produce Fe-functionalised catalyst pellets was established. In this way, large quantities of catalyst pellets (>200 g) could be produced, installed in the in-house high-pressure apparatus, and tested in CO_2 methanation. A sorption-enhancement effect was measured. For the Fe-based system at hand, the enhancement depends not only on pressure and temperature but also on factors such as the Fe precursor used in the material preparation. Monometallic Fe-catalysts seemed prone to a phase change during methanation, and a persistent Fe-carbide phase was identified by X-Ray diffraction (XRD). The addition of cobalt led to a better performance with a maximum conversion of ~100% with a CH_4 selectivity of up to 97%. Furthermore, the first investigations on the degradation of the materials were carried out and the Co-doped material presented a stable performance in up to 10 reaction cycles with no carbon accumulation as indicated by the Thermogravimetric analysis results. The achievements of this project increased the maturity of the sorption-enhanced methanation technology, which now can be operated in quasi-continuous mode with non-noble metal catalytic materials with a lower impact on the environment.

Main findings

- For the first time, iron-zeolite catalysts were reported as successfully active for CO_2 methanation
- An ion-exchanged iron-based material, free from noble metals was successfully developed and a novel synthesis procedure was established
- A reduction of about 80% in the metal content was achieved, compared to most conventional nickel catalysts
- Bimetallic CoFe material demonstrated high stability for conversion and selectivity maintained over 10 reaction cycles (methanation/regeneration)
- Bimetallic CoFe material was resistant to carbon accumulation which is one of the main causes of deactivation in methanation systems

Contents

Abbreviations

DFT	Density Functional Theory
EDTA	Ethylenediaminetetraacetic acid
GC	Gas chromatography
GHSV	Gas Hourly Space Velocity
HEPP	High-Efficiency Power-to-Methane Pilot
IR	Infrared
LD50	Lethal dose, 50%
LOM	Light Optical Microscopy
LRV	Luftreinhaltung
MAK	Maximale Arbeitsplatz-Konzentration
MFC	Mass Flow Controler
MS	Mass spectrometry
PtG	Power-to-Gas
SEM	Sorption Enhanced Methanation
SFOE	Swiss Federal Office of Energy
TGA	Thermogravimetric Analysis
TPR	Temperature Programmed Reduction
TRL	Technology Readiness Level
XRD	X-ray Diffraction
XRF	X-ray Fluorescence
WP	Work Package

Since the start of the SmartHife[2] project in 2020, the nickel price doubled reaching the value of 21233 USD/ton in June 2023 (Figure 1). Despite the nickel market price over the years being driven by demand and supply shocks, the recent conflicts in Eastern Europe impacted harshly the prices that suffer the biggest fluctuation in 10 years. Therefore, alternatives to circumvent the nickel dependence in industrial processes, like the one proposed in this project, are very welcomed.

1 Introduction

1.1 Background information and current situation

Switzerland offers biogas sources – with an available energy output of 400 GWh, and the potential is far from being fully exploited, the total usable energy output is about 28 times greater (SFOE,2021). Additionally, the Swiss gas industry aims for a massive increase of renewable methane (CH_4) in the Swiss market by up to 30% in 2030. Common biogas sources (i.e. fermenters) are usually operated at low temperatures, atmospheric pressure, and low gas hourly space velocities (GHSV). Gas mixtures from such sources need to be compressed and heated to be upgraded with conventional catalysts, which causes an important operation parameter to shift in the production process.
Studies, recently performed in the frame of sorption-enhanced methanation process enables the continuous production of pure 100% CH_4 at low temperature and pressure levels compared to classic methanation catalysts. An important difference between this new process and classic catalysts is the low GHSV required (by orders of magnitude), to allow for a stable waterfront to propagate through the reactor (Borgschulte et al., 2016). Although this would normally be seen as a drawback, this becomes an advantage if a sorption-enhanced methanation plant is connected to biological plants, such as a fermenter: the close operation parameters of both technologies allow building a continuous process on-site. Additionally, there are two major drawbacks to direct application, which require further development. Firstly, sulfurous gases present in biogas sources strongly hinder the catalytic activity of nickel-based methanation catalysts. Secondly, the price of nickel (Ni) compared to other power-to-gas catalysts like iron (Fe) and Copper (Cu) (Table 1):

Table 1 - Prices of metal catalysts for power-to-gas applications (source: Insider Business as of Jun 31, 2023).

Metal	Price (USD/Ton)	Price ratio
Fe	112	1
Cu	8651	77
Ni	21233	189

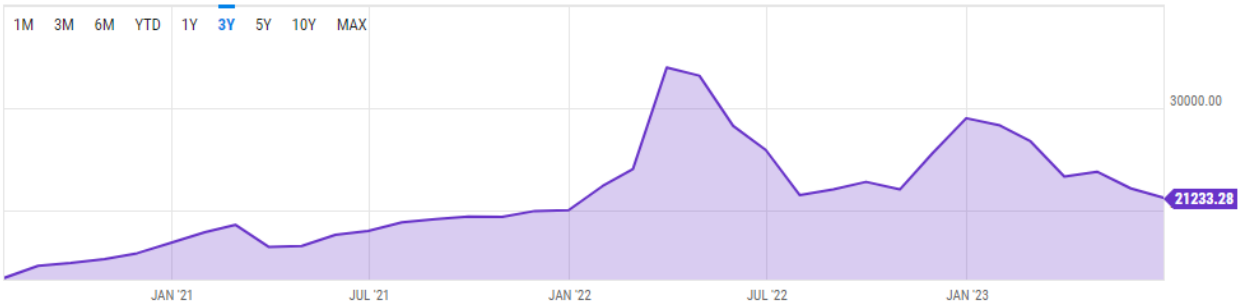

Figure 1 - Nickel price chart in USD/ton from 2020 to 2023. Source: YCharts.Inc.

1.2 Purpose of the project

This project aims the development of a new generation of sorption-enhanced methanation catalysts. The former generation, which is based on Ni as the catalytically active metal has proven the high efficiency and scalability of sorption-enhanced catalysis. Now the development of a new, iron-based generation to tackle the remaining obstacles towards industrialization involves further fundamental and technological improvement and the objectives can be summarized as follows:

- Application of a more cost-effective **Fe catalyst** with reduced ecological and human toxicity (LD_{50}, "MAK" or exhaust values according to LRV in Switzerland) for a biogas upgrade by sorption-enhanced methanation
- Increasing the catalyst activity on the base of Fe and identification of **optimal operation conditions** (pressure, temperature) and in-depth understanding of selectivity, conversion rate, and CH_4 yield of the sorption-enhanced process on Fe
- exploration of **catalytically active sites** by doping Fe with highly active metals (Ni, Ru)
- Enable an effective **continuous operation** by **optimization of regeneration times** (drying phase).
- Increasing the catalysts' **stability** or degradation rate (in %/100 h) by identification of degradation mechanisms (e.g. pressure, hydrothermal treatment, metal incorporation) and suitable countermeasures
- Evaluation of the **sulfur tolerance and robustness of sorption-enhanced methanation catalysts** at relevant biogas qualities
- **Increase of TRL** by evaluation of technologic and scientific criteria to state-of-the-art and cost-performance correlation by implementation and **operation in the OST demonstrator plant (proof of concept)**

1.3 Objectives

The main objective of this project is the development of highly efficient sorption-enhanced methanation technology for a biogas upgrade. The project was divided into different work packages containing all qualitative and quantitative objects that were achieved in the project and all of them are described below:

WP1: Sorption-enhanced Fe-based catalyst design

The objective of this work task is the development of a Fe-based catalyst concept for sorption-enhanced methanation. Investigation of the Fe-based concept and optimization of the performance within sorption-enhanced methanation reaction by structure-performance correlation is the most crucial aspect and the main goal. Especially, since Fe is less prone to typical biogas contaminations such as sulfur, but lacks performance and selectivity compared to Ni as the state-of-the-art catalyst.

WP2: Efficient Catalyst regeneration by microstructure design

A vital balance between methanation and regeneration times is crucial for the continuous operation of the catalyst within a fixed-bed reactor. For processed sorption-enhanced catalysts, that typically possess a spheric or cylindric pallet shape, the regeneration, i.e. drying from adsorbed water, has been shown to be non-linear and strongly diffusion dependent. As a result, the regeneration time is longer compared to the methanation time. Hence, this work task aims to shorten regeneration times by optimizing the elimination of water through the introduction of additional open porosity into catalyst pellets.

WP3: Stability & degradation during sorption-enhanced methanation

The objective of this work task is to investigate the performance of the optimized Fe-based sorption-enhanced catalysts over 100 h operation and/or 10 cycles. Various effects like metal deactivation or loss of porosity can lead to the degradation of the catalysts during long-time operation. Those mechanisms must be identified and need to be avoided by correlated countermeasures in order to successfully apply the catalyst for the biogas upgrade.

WP4: Technology Assessment, Dissemination, and Know-how Transfer

The objective of this work task is the assessment, dissemination, and know-how transfer of SmartHiFe^2 results from a scientific and more important technological perspective. This is on the one hand, a proof-of-concept of SmartHiFe^2 materials in the research platform HEPP and on the other hand a know-how and technology transfer of the sorption-enhanced technology to industrial stakeholders and system integrators for industrial use. A TRL shift of this Fe-based technology from 2 to 5 or even 6 (industry plant in biogas environment) is expected.

2 Description of facility

Not valid here, but the catalytic test setup description is integrated into Section 3.

3 Procedures and methodology

3.1 Material design

Along the project's advance, much was made in terms of material development. At the beginning of SmartHife^2, we strategically chose to pursue the synthesis method developed in SmartCat (Delmelle et al., 2016). New findings led us to develop a new method for zeolite functionalization that presented better results. Therefore, we divided the iron-based materials into the following two classes:

a) The first generation of iron-based materials: Based on the SmartCat approach (Delmelle et al., 2016)
b) The second generation of iron-based materials: newly developed synthesis method

3.1.1 The first generation of Fe-based materials: Powder x Pellets

Due to the promising results from preliminary experiments (Franken & Heel, 2020) zeolite 13X was chosen in its pelletized form as support. An infiltration procedure was used for the functionalization with Fe, which has been proven as very straightforward and efficient in the former SFOE project SmartCat (SI 501130-01) for Ni-based systems (Delmelle et al., 2016). Table 2 describes the chemicals used for the Fe-infiltration procedure as well as the Fe content and nomenclature:

Table 2 - Chemicals used in the preparation and nomenclature of the materials.

Fe Precursor	Chem. Formula	Fe content (w.t.%)	Solvent	Nomenclature
Iron(II) Sulphate	$Fe(SO)_4$	1	Water	Fesul13XW
Iron(III) nitrate nonahydrate	$Fe(NO_3)_3 \cdot 9H_2O$	1	Water	Fenit13XW
Iron(III) nitrate nonahydrate	$Fe(NO_3)_3 \cdot 9H_2O$	1	Ethanol	Fenit13XE

An alternative to obtaining Fe-functionalized catalyst pellets is to use the zeolite as a powder instead of commercially available pellets. The powder is functionalized by impregnation with the catalytic active element and afterward subjected to pelletization. In this way, the properties of the pellets, such as porosity, size, and shape, can be specifically adapted which is important to shorten regeneration times (removal of water) from the zeolite pellet. In addition, diffusion effects, which occur during infiltration due to the relatively long distances from the outer pellet to the inner core, can be avoided. The same is valid for the water removal as a reaction product from the CO_2-methanation reaction. Also, the strong dependence of infiltration on certain Fe precursors (in this case Fe(II)-sulfate) in order not to destroy the pellets (e.g. by dissolution of the present binder) can be eliminated.
For the powder infiltration, a corresponding amount of $Fe(NO_3)_3$ in ethanol was used to obtain a total Fe concentration of 1 wt% (related to the zeolite mass). Instead of calcination, the functionalization is followed by a pelletization step. For this, the Fe-functionalised powder is mixed with a binder (Al_2O_3), a pore-forming agent (potato starch), and moistened with acetic acid. An extrusion aid (hydroxymethyl cellulose) is added to obtain the right kneadable consistency for extrusion. The extruded pellets are dried, broken down to the appropriate size by a mill, and subsequently sieved to obtain a homogeneous sample fraction with a pellet diameter of d ~ 1 mm.
In summary, for the first material generation, two different approaches (Figure 2) for the synthesis of iron-based sorption-enhanced catalyst pellets were pursued. In the first approach (A), following the example of the Ni-based catalyst generation (Delmelle et al., 2016), we used zeolite pellets as starting material. The developed three-step process involves:

a) Infiltration of the iron species into the pellets
b) Calcination of decomposable residues by an oxidation step
c) Activation of the metal catalyst by a reduction step

In approach (B) the zeolite is initially used in a powder form. As a result, an additional pelletization step follows the infiltration to use the catalyst in the catalyst bed. Thus, (A) has the advantage of lower process costs, since this approach has fewer production steps when compared to (B), whereas (B) is by far more flexible regarding the infiltration and composition of the pellets (shape, size, porosity).

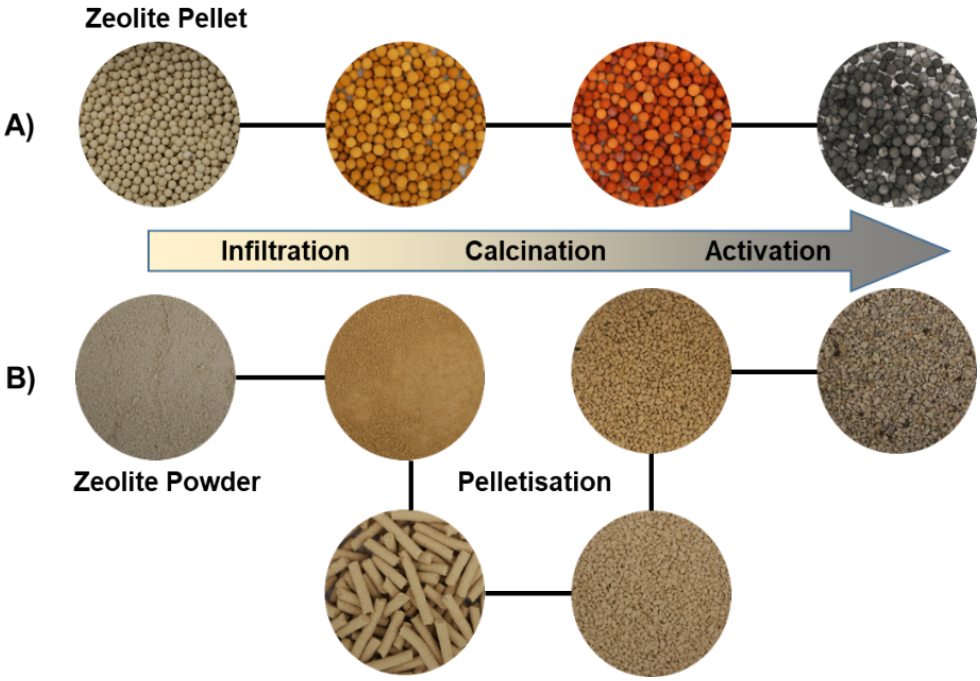

Figure 2 - Overview of two different approaches for the synthesis of Fe-based catalyst: A) Infiltration of commercially available 13X zeolite pellets. B) Infiltration and pelletization of 13X zeolite powder.

3.1.2 The second generation of iron-based materials: newly developed "water-free" infiltration

From a catalyst synthesis point of view, it follows that the more uniform the catalyst is, the higher the probability of being able to interpret the performance data obtained unambiguously. From the first phase, it is known that Fe-based materials are significantly more difficult to reach homogenous and well-performing pellets. At that time no clear strategy was available to succeed with such a challenging system. Approaching this challenge, the first step to establishing a well-performing material is to understand and define a reliable synthesis route. As described above, Fe precursors can play a key role in the synthesis governing the Fe species homogeneity of the final material. But this is not the only parameter that should be considered, Figure 3 shows two different possible metal-containing zeolites.

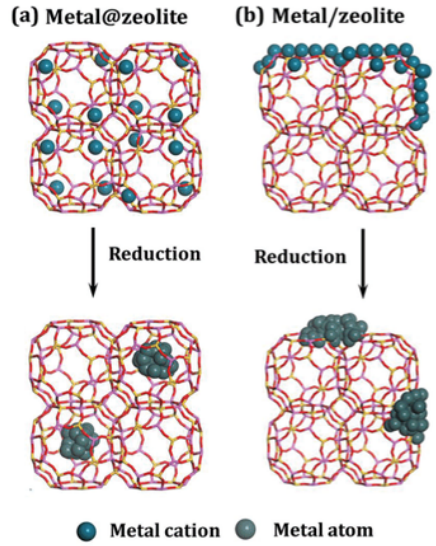

Figure 3 - Different possibilities for metal-containing zeolites prepared by infiltration: a) Metal@zeolite and b) metal/zeolite. Source: adapted from (Chai et al. 2019).

As seen in Fig. 3 the preparation method will define the metal distribution, as well as the cation size which is governed by the metal precursor. Depending on the metal cation (type/size) it is possible to generate “metal@zeolite” (Fig.3a), which after thermal treatment in a reductive environment, results in metal atoms dispersed in the zeolite cavities. Or “metal/zeolite” (Fig.3b) which results in agglomerated metal species over the zeolite surface after treatment. It is well known from the literature that agglomerated metal species present poor catalytic activity when compared to highly dispersed metal species, so careful consideration of the synthesis method is crucial for a well-performing material design. Based on the SmartCat approach (Delmelle et al., 2016; Delmelle et al., 2018), it was possible to synthesize homogeneous Ni-zeolite materials using an aqueous infiltration procedure. The Ni speciation in aqueous medium (Figure 4) generates only Ni^{2+} cations which are favorable for the synthesis of “metal@zeolite” (Fig.3a) materials, resulting in a homogeneous Ni distribution within the zeolite.

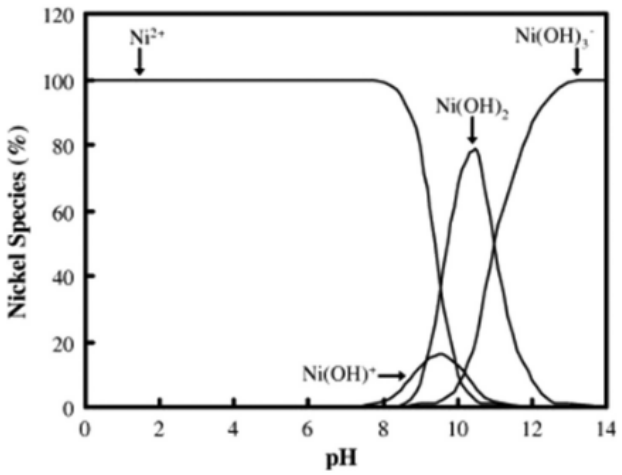

Figure 4 – Ni speciation in aqueous medium versus pH. Source: (El-Naggar et al. 2021).

On the other hand, the Fe speciation in aqueous medium is completely different as shown in Figure 5.

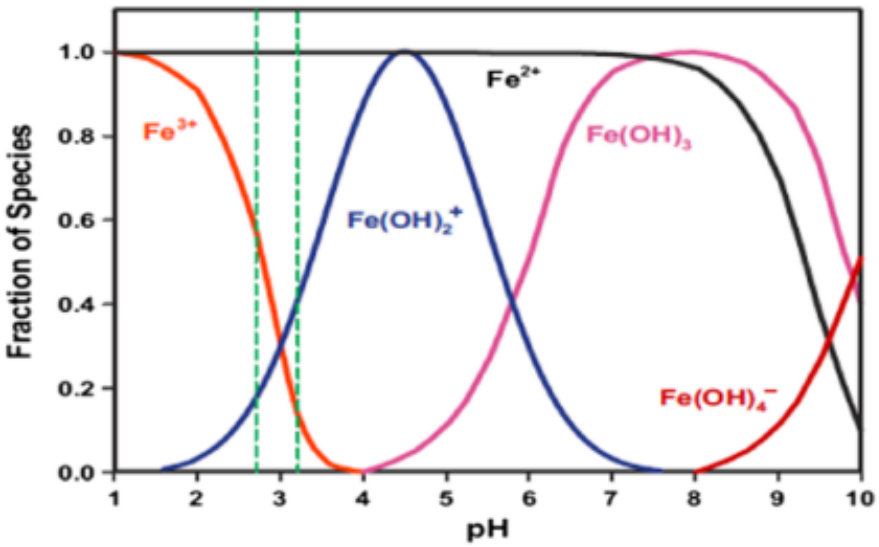

Figure 5 - Fe speciation in aqueous medium versus pH. Source: (Xing et al., 2017).

The Fe speciation in the aqueous media diagram (Fig.5), differently from Ni (Fig.4) shows the presence of four different species, Fe^{3+}, Fe^{2+}, $Fe(OH)_2^+$, and $Fe(OH)_3$ which give much complexity to the synthesis of Fe-zeolite materials which tends to result on the materials described in “metal/zeolite” mechanism (Figure3b). This is related to the fact that bigger cations such as hydroxyls favorably stabilize on the zeolite surface for not being able to fit into the zeolite cavities. Partial precipitation of insoluble Fe hydroxides in the solution may also occur making the infiltration process inefficient. Therefore, knowing how to control Fe speciation could be the key to material design. Metal speciation can be controlled by the dissolution in different mediums, pH, and metal precursors. Hereby, we proposed the use of a water-free infiltration procedure using different Fe precursors chosen accordingly to the compatibility with the zeolite and Fe oxidation state. Table 3 describes the chemicals used for the Fe-infiltration procedure and also includes the materials' nomenclature. Zeolite 13X (Zeochem) was used as the base material.

Table 3 - Chemicals used in the preparation and nomenclature of the materials.

Fe Precursor	**Chem. Formula**	**Fe content (w.t.%)**	**Solvent**	**Nomenclature**
Iron(0) pentacarbonyl	$Fe(CO)_5$	1	Toluene	Fecarb13XT
Iron(II) acetylacetonate	$[CH_3COCH=C(O)CH_3]_2Fe$	1	Toluene	Feacac13XT
Iron(III) nitrate nonahydrate	$Fe(NO_3)_3 \cdot 9H_2O$	1	Methanol	Fenit13XM

After the infiltration procedure, all the materials were dried overnight at 120°C and calcined in static air at 500°C for 12 hours.

3.2 Catalytic test setup

On a technical level, high-pressure catalytic screening on pellets in the sorption mode is a crucial aspect of the SmartHiFe^2 project. A high-pressure operation reactor was built and allows to perform the methanation on a scalable size at pressures up to 65 bar and the up-to-date results will be presented in Section 4. Additionally, our partner Fluitec has provided a semi-industrial and scalable reactor concept with d = 0.12 m and l = 1 m, resulting in a total volume of 6.8 L (~5 kg catalyst) which is also certified for pressure operation (Figure 6). This reactor concept is scalable up to several m^3 of volume and diameter up to 2 or 3 m as well as several meters in length. In general, the reactor can be used up to 100 bar, but it was limited to 65 bar due to the costs of the certification process and the lab infrastructure (MFC and pressure lines). A notable fact is here, that a new silicon oil heat transfer system is used in combination, which is applied to avoid formerly seen hot spots, reducing the material performance. Furthermore, proper heat insulation was recently acquired, bringing the system even closer to an industrial plant level. Since an adequate reactor and heat exchange setup for catalytic testing is a crucial part of this project, a reliable setup allows the extraction of the parameters for a real operation leading to easier knowledge transfer for industrial partners. Furthermore, such a robust and large reactor as the one from Fluitec (Figure 6) is nowhere to be found in another lab facility, allowing us to come from a lab scale to a realistic scenario. In principle, this system can be seen as operating in an industrial setting, except for the fact, that the reaction heat is not re-integrated in a plant setting and the methanation process is independent of that fact.

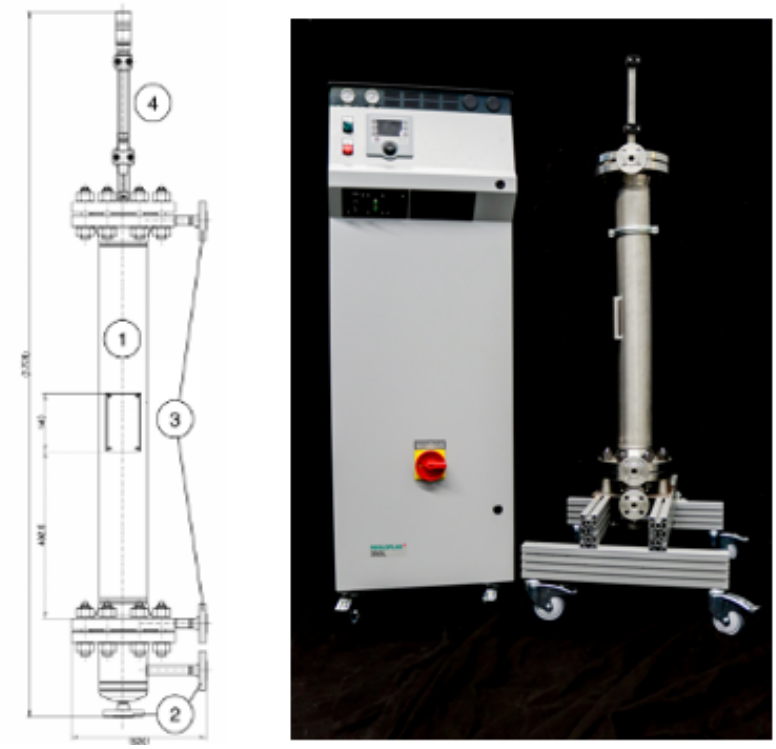

Figure 6 - Semi-industrial reactor provided by Fluitec, Switzerland (left), including the drawing (right) of: 1) reactor tube; 2) thermal oil in- and outlet; 3) gas in-and outlet; 4) thermocouple.

3.3 Operational conditions

Many parameters such as operation conditions: temperature, pressure, flow rates, as well as catalyst pre-treatment, activation conditions, etc., influence the performance of heterogeneous catalysts in the methanation reaction. For systematic investigations and optimizations, it is essential to reach the best-performing catalyst and operation conditions. Secondly, such a precise and reliable set of operational conditions is needed to be scaled up and transferred to our industrial partner for later industrialization. Therefore, we have screened different parameters for the methanation reaction such as pressure, temperature, and activation conditions, as exemplified in Table 4, which were meticulously chosen according to previous sample characterization:

Table 4 – Reaction parameters used for the catalytic screening.

Sample	Activation Temperature (°C)	Reaction temperature (°C)	Pressure (bar)
Fenit13XW	400, 450	400, 450	1, 6, 16, 21
Fesul13XW	400	400	1, 6, 16, 21
Feacac13XT	400	250, 300, 350, 400	1 and 15
Fecarb13XT	400 and no activation	400	15

4 Results and discussion

4.1 Results on the first generation of Fe-based zeolite materials

As described in the previous section as approach A (Figure 2a), an infiltration procedure was used for the functionalization of the zeolite pellets with Fe, which has been proven as very straightforward and efficient in former methods for Ni-based systems. However, due to the different properties of Fe precursors (e.g. cation diameter) compared to Ni ones, formerly elaborated synthesis routes could not be applied here. Direct transfer and application of functionalization routes result in the structural degradation of the zeolite pellets, which is apparent by the detachment of outer pellet layers (Figure 7a). One possible reason is the higher acidity of iron (III) ions in an aqueous solution (pH ~2), which results in the dissolution of the alumina from the zeolite network.

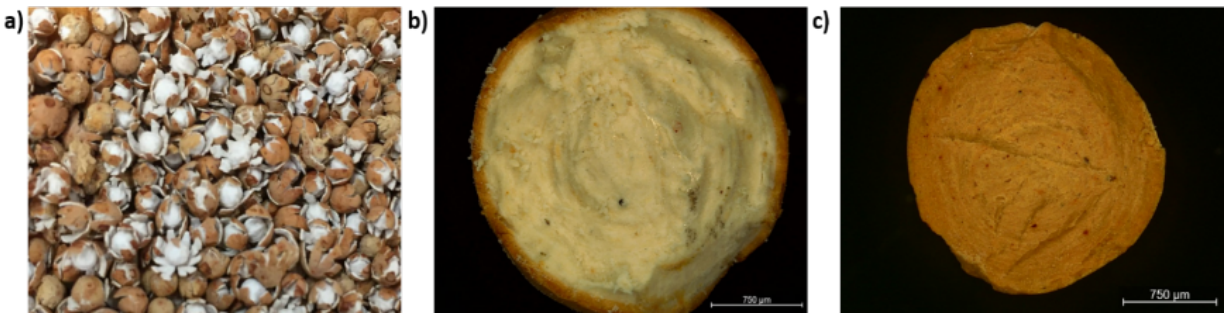

Figure 7 – Images of the Fe-functionalized zeolites: a) optical image of destroyed zeolite pellets after the functionalization with Fe by the Ni-standard protocol; b) LOM Cross-sectional images of single pellets after functionalization in ethanol and c) according to the optimized conditions.

In addition, the dissolution of the used binder (typically bentonite) used for the pelletization could be another origin for the disintegration of the macrostructure. Consequently, the solvent was initially changed to ethanol. Ethanol is less protic and is known from preliminary studies to result in better functionalization results. Figure 7b shows the cross-section of a single zeolite pellet infiltrated for 24h in a 0.05M Fe-(III)nitrate solution received by optical microscopy. A colour gradient from orange (outer layer) to sand colour (core) can be seen across the pellet, which indicates a Fe-functionalization with a detrimental core-shell distribution. Increasing the concentration of iron precursor in ethanol (1M) leads on a short-term scale to the degradation of the pellets and on a long-term scale to a massive and counterproductive gelation of the solvent.

In order to still achieve a homogeneous functionalization, further experiments with different Fe precursors such as phosphates or sulfates, etc. were carried out with variable solvents (e.g. water, alcohols, ethers, etc.). From this highly necessary pre-study, optimal parameters could be found for a homogeneous distribution of Fe within the commercially available zeolite pellets. These parameters are a 3h infiltration in an aqueous 1M Fe(II) sulfate solution (pH ~4) is used and shows the best reproducibility. The cross-section of such a pellet (Figure 3c) shows a homogenous colour distribution without any core-shell structure visible. Additionally, a second approach is where the zeolite is initially used in a powder form. As a result, an additional pelletization step follows the infiltration in order to use the catalyst for catalytic testing.

Preliminary catalytic investigations in the kinetic tube reactor have shown that Fe(II)-sulfate infiltrated commercial pellets (approach A, Figure 2A) have no activity towards CH_4 formation. Although different reaction conditions like higher temperature, different H_2/CO_2 ratios as well as different flow rates were probed the catalyst was not active. Investigations are ongoing but the assumption is made that sulfur is not removed completely by the calcination procedure of the precursor and is blocking the catalytic centres. XRF measurements confirm the ratio of Fe to S to be in the range of 7: 1. For further investigations regarding sorption-enhanced methanation, only material produced according to approach B (infiltration of zeolite powder with Fe(III)-nitrate) was used. The high-pressure reactor (d = 3 cm, L = 50 cm) was used for the experiments. For its filling, about 140 g of catalyst material was prepared, pelletized, and installed in the catalyst bed. For methanation, a mixture of H_2 and CO_2 (ratio 4.05) with a GHSV of 100 was passed through the reactor. The analysis of the products was done online with a mass spectrometer. Figure 8a shows the signal data of a typical reaction sequence (p = 5 bar, T = 450°C). These can be divided into two segments: 1) sorption segment and 2) equilibrium segment. As soon as the adsorption capacity of the zeolite is reached (pores filled with water; sorption stage), the thermodynamic equilibrium of the methanation reaction is achieved. This is recognized by an increase in CO_2 concentration and thus a decrease in conversion (<100%). This behaviour is given in the measured data. After switching on the reaction mixture (t = 0), the inert gas (Ar) used is measured first due to the low exchange rate. From t = 413 s a clear change occurs as product gases, CH_4 and CO, and excess H_2 can be detected. From t = 672 the CO_2 content in the exhaust gas increases. The conversion decreases to approx. 45% and thus also the proportion of CO and CH_4 in the exhaust gas. Further pressure-dependent measurements have shown a similar behaviour (Figure 8b). In all measurements (up to p = 21 bar) the sorption effect could be measured. The CO_2 conversions are similar. However, there is a change in the product distribution between CO and CH_4. With increasing pressure, the selectivity of the reaction shifts in favour of CH_4 and seems to reach a maximum of ca. 43% at p = 16 bar. It can also be seen that the selectivity for CH_4 in sorption mode is slightly higher than in the equilibrium case.

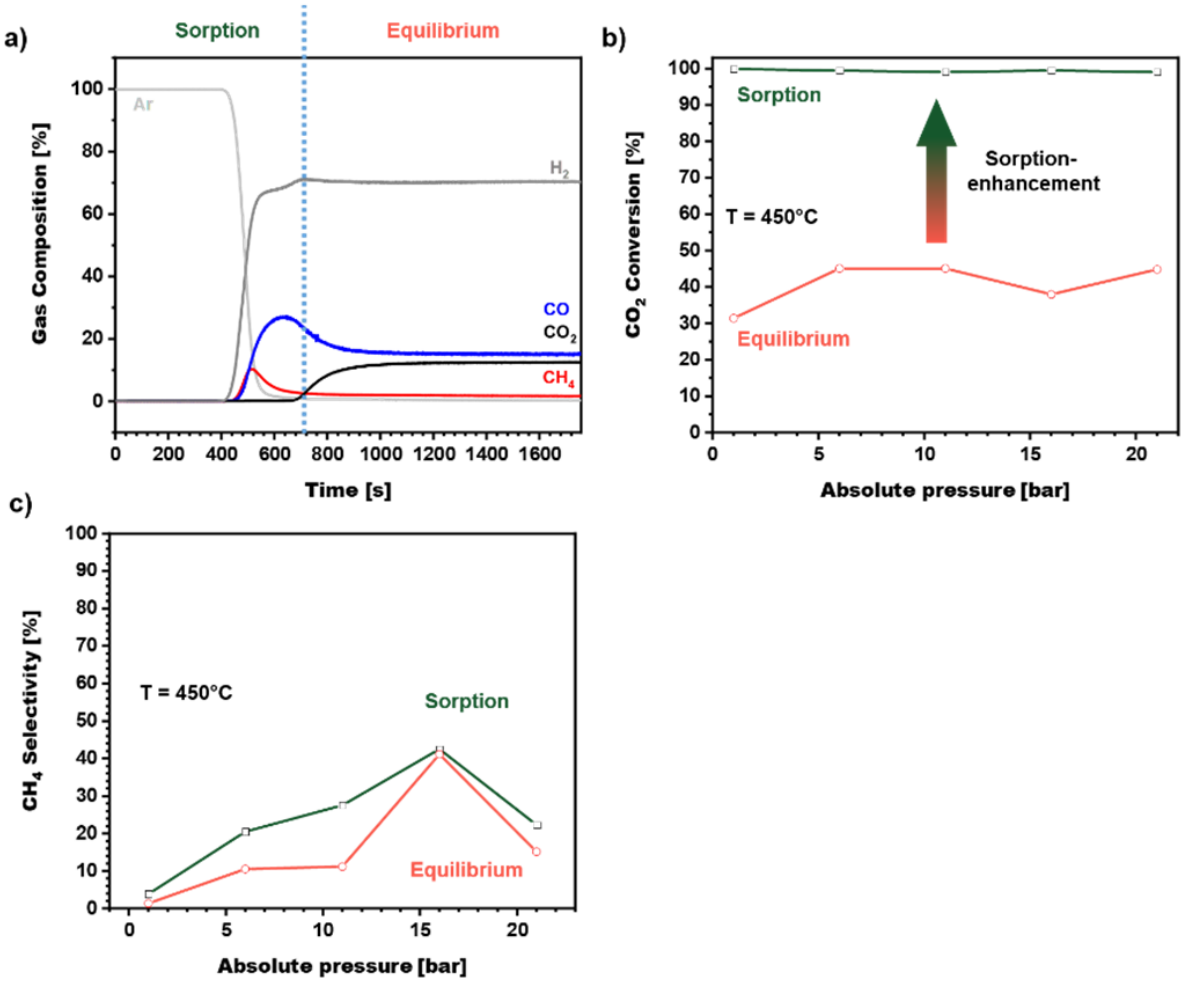

Figure 8 - a) MS-Data of a typical methanation run (p = 6 bar; T = 450°C) on 1wt% Fe-functionalized zeolite 13X. b) CO_2 conversion as well as c) CH_4 selectivity of pressure-dependent methanation runs at T = 450°C determined for the sorption (green) as well as the equilibrium state (red) of the reaction.

As observed in Figure 8b and c, in terms of CO_2 conversion and CH_4 selectivity an operating pressure of 15 bar can be considered as the optimal reaction pressure. For this reason, from now on, all the catalytic testing will be conducted at 15 bar.
As planned for WP2, the insertion of open porosities (meso/macro) into catalyst pellets may improve water transport from zeolite, facilitating the water transfer in the pellets and helping to reach a 1-to-1 time ratio between methanation and regeneration (drying). To accomplish so, two methods to increase inner porosity were applied:

1) Acidic/basic etching
2) Pelletizing procedure using a template

In the first case, the generation of meso/macro pores via an etching procedure in the material can be done in two steps: dealumination and/or desilication (Verboekend et al., 2012). For dealumination, the zeolite powder is mixed with an aqueous H_4-EDTA solution (acidic etching). The EDTA etches aluminium from the zeolite structure, thereby the procedure is relatively mild compared to the use of inorganic acids. In order to create a homogeneous structure again, silicon is also released from the structure in a second step. This is done by treatment with an aqueous NaOH solution (basic etching). To remove amorphous

or precipitating aluminium oxide, a third washing step with Na_2-EDTA is carried out. To verify if the etched material can still be Fe functionalized according to the developed procedure (approach B, Figure 2B), the etched material was functionalized with Fe(III)-nitrate and pelletized in a final step.

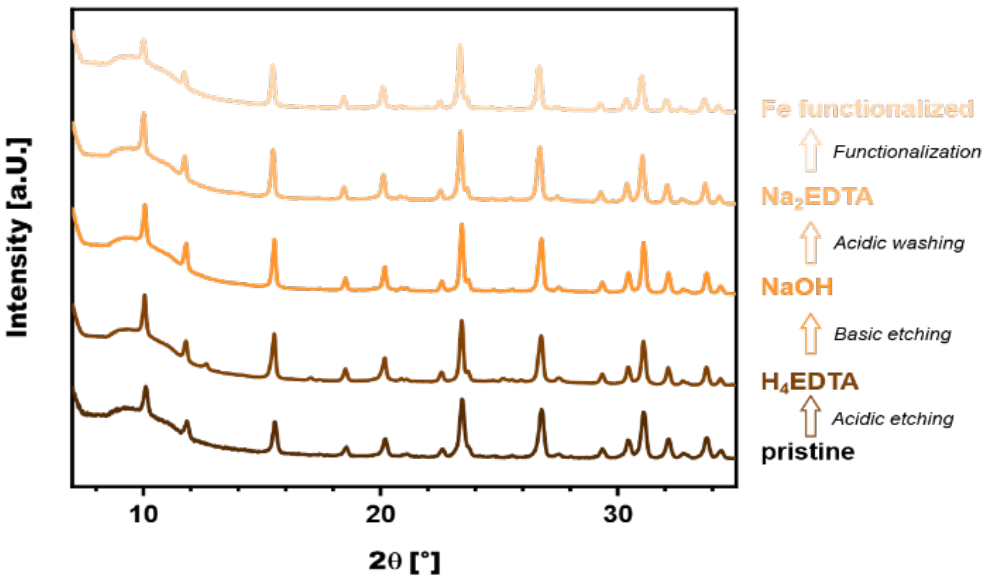

Figure 9 - XRD analysis of crystalline structure after different steps of acid/basic etching.

XRD was used to examine whether the crystalline structure was preserved after the individual etching steps (Figure 9). The recorded diffractograms do not show any visible differences, it is therefore assumed that the crystalline structure is not affected by the etching process. The subsequent functionalization with Fe does not seem to have a negative influence on the crystal structure either, as the pattern does not change noticeably.

In order to examine the changes in porosity in more detail, N_2-physisorption measurements of the samples were carried out (Figure 10). From the adsorption isotherms (Figure 10a), it can already be seen that the proportion of micropores decreases overall as the etching procedure progresses. This is indicated by the reduced adsorbed volume at low pressures ($p<0.2$). Compared to the pristine material, the isotherms show a hysteresis at higher pressures. As already discussed for the pelletization process, this indicates the generation of meso/macro pores. For the size range of the zeolite pores, a pore size distribution was made using DFT calculation (Figure 10b). According to this, the original pore size of the 13X is ~0.9 nm. While etching, the pores widen to ~1 nm. It is interesting that the Fe-functionalised materials again have smaller pores. The surface area, the proportion of micropores, and the external surface area (meso-/macro pores) are listed in Table 5. As expected, the total surface area decreases from 696 m^2g^{-1} to 358 m^2g^{-1}, but the proportion of external surface in the material increases. Thus, a more open porosity could be generated by the etching procedure due to the higher proportion of external surface (process schematically drawn in Figure 10c).

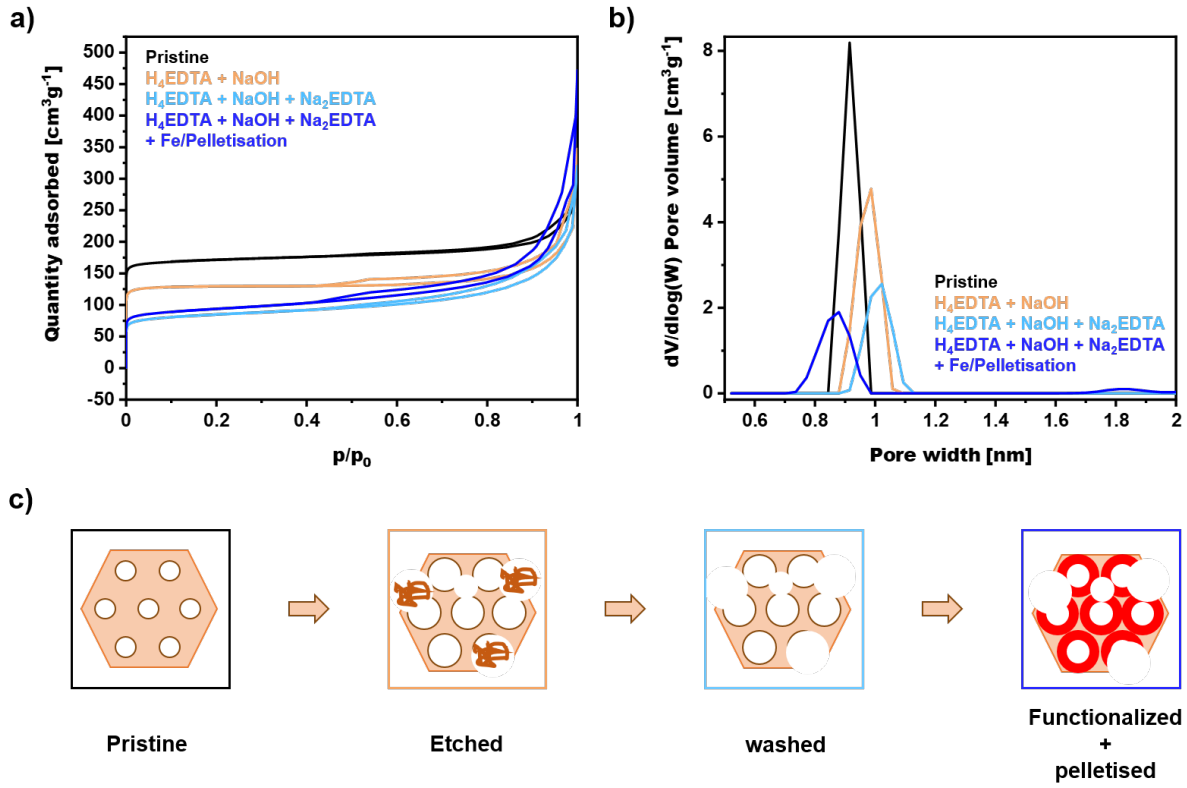

Figure 10 - N_2-Pyhsisorption measurements on: a) different stages of the etching procedure; b) isotherms; c) DFT-pore size calculation and schematic illustration.

Table 5 - BET and percentage of micropores determined for different etching steps.

Form	13X	13X H_4EDTA NaOH	13X H_4EDTA NaOH H_2EDTA	13X H_4EDTA NaOH Na_2EDTA Fe/Pellet
BET [m^2g^{-1}]	696	532	323	358
Micropores	91%	94%	72%	65%
External Area [m^2g^{-1}]	66	31	91	106

Even though the material porosity was successfully generated, no activity towards methanation was observed, it can be assumed that the removal of external Al species, which would not be observed in the XRD measurements, can lead to different Fe species after infiltration procedures that are inactive for methanation and/or in a change in the material acidity resulting in poor activity (Shetti et al., 2008). The second method used to insert inner porosity into the materials was a pelletizing procedure using a template. In the pelletization process developed (Figure 2B), potato starch was used as a template to

form open porosities. The starch acts as an organic sacrificial substrate, which can be removed by a calcination (in air) step without leaving any residue. The calcination process creates voids in the material, which contribute to the open porosity. Methanation tests at p = 15 bar and T = 350°C show a strong dependence of the performance of the system (potato starch as pore former) on the drying time (Figure 11). Three cycles are shown, whereby the second cycle was carried out after 1 h drying time and the third cycle after 12 h drying time. If only the products are considered, the CH_4 concentration initially increases in the first cycle. After ca. 70 s the CO concentration increases and finally, after 180 s the CO_2 concentration increases, which marks the end of the sorption phase. In the second, the concentrations of the product gases (CH_4 and CO) increase almost simultaneously with the CO_2 concentration. A sorption phase is thus basically non-existent. In the third cycle, after 12 hours of drying time, the CH_4 concentration rises first. After 130 s, the CO follows, and after 270 s the CO_2 breaks through. Due to the longer drying time, at least the initial capacity could be restored.

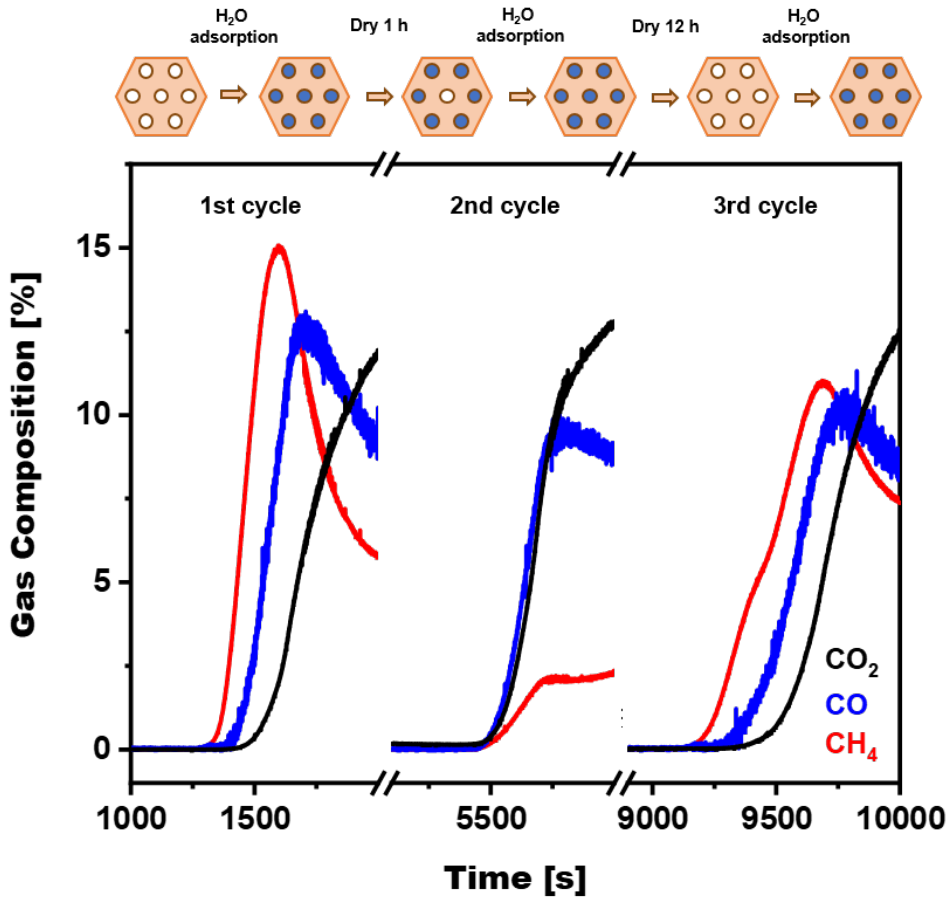

Figure 11 - Methanation cycles with different drying times at p = 15 bar and T = 350°C with potato starch as a pore-forming agent (H_2 and Ar Signals not shown for better clarity). Schemes indicate the filling of pores with water.

These results indicate that even though the material's porosity increased, its water sorption and desorption capacity showed not to be improved. A different approach is therefore required, and it will be discussed in the next sections.

4.2 Results on the second generation of Fe-based zeolite materials

As significant progress in the material design was made and it was clarified how the synthesis mechanisms for Fe-containing zeolites work (as described in Section 3.1), the authors strategically opted for the pellet approach, which is commercially available and ready for Fe infiltration with no further steps required. The new materials resulting from the water-free pellets infiltration are shown in Figure 12:

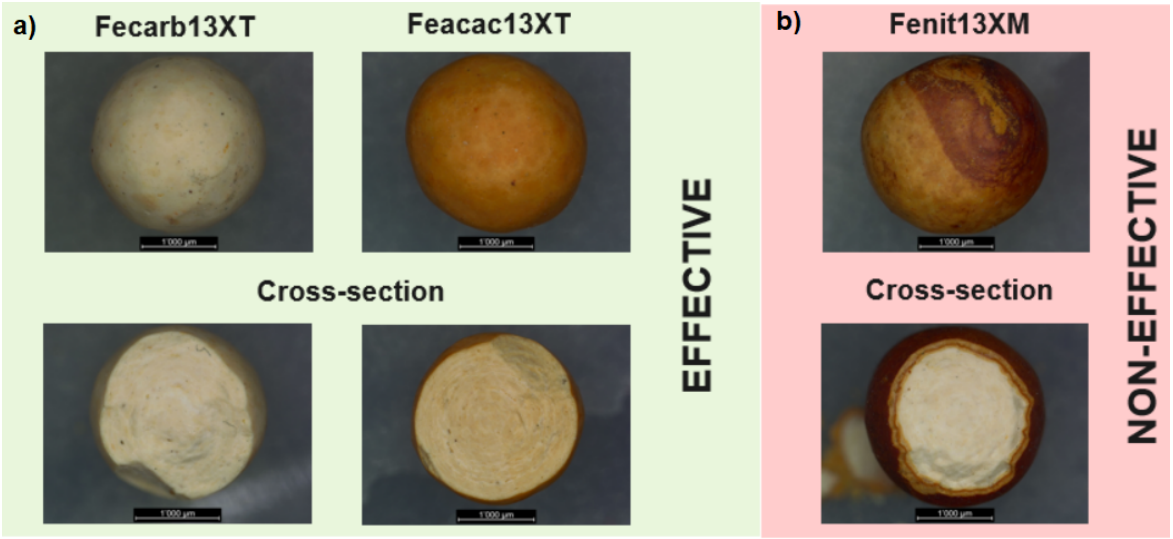

Figure 12 - LOM images from the pellets prepared by water-free infiltration: a) Toluene as the solvent, and b) Methanol as the solvent, and respective cross sections.

The Fecarb13XT (carb = carbonyl on 13X Zeolite, T = toluene) and Feacac13XT (acac = acetylacetonate) samples (Fig. 12a) infiltrated using Toluene as solvent show a homogeneous colour through the pellet (see cross-section). It is well known that the orange colour of Fe compounds is related to Fe(III) oxide and hydroxides, and it is even intensified in an oxidative environment (Pfaff, 2021). Nonetheless, the different colours seen for Fecarb13XT and Feacac13XT are related to the different oxidation states of the Fe precursors. For instance, Fecarb13XT was prepared using iron(0)pentacarbonyl precursor while Feacac13XT sample with iron(II)acetylacetonate. On the other hand, for the Fenit13XM sample (nit = nitrate, M = methanol, Fig. 12b), it is observed that the infiltration procedure was not effective. The Fe species were concentrated on the outer sphere being unable to penetrate the pellet (c.f. cross-section).

As mentioned in section 3.1 depending on the precursor and pH the Fe speciation can be different, and the precipitation of oxides and hydroxides may occur, and those species tend to accumulate over the pellet surface being unable to penetrate its pores. For the Fenit13XM (Fig. 12b), the solvent used was methanol (CH_3COH), due to the chemical compatibility with the Fe precursor, and with alcoholic solutions, it is very hard to keep a water-free environment, thus, precipitation of Fe hydroxide may occur explaining the strong orange colour in the outer surface of the pellet.

Previous results indicated that the synthesis method has a significant impact on the zeolite macro- and microstructure being the cause of the structure collapse and lack of performance. Therefore, XRD measurements were performed to characterize the material's structure after the Fe infiltration procedure (Figure 13):

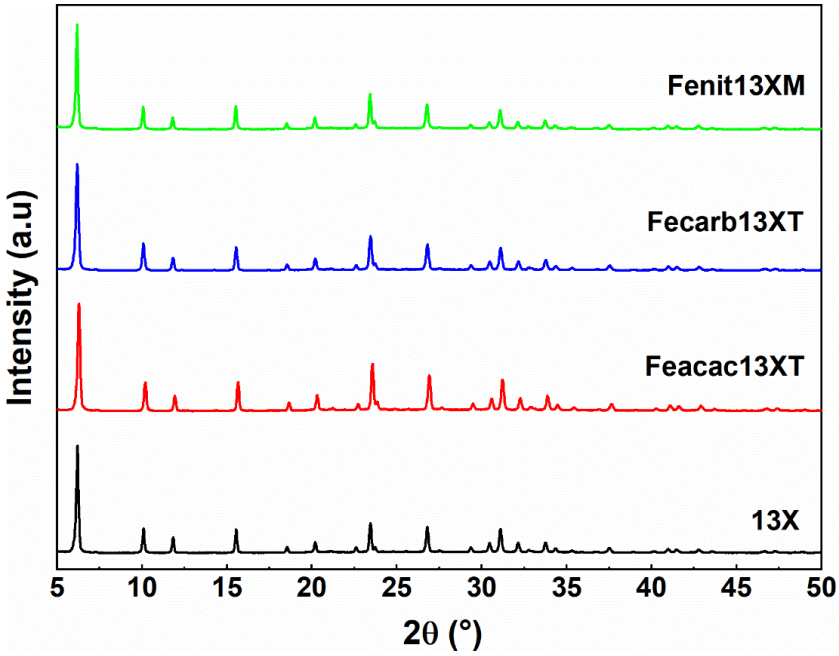

Figure 13 - Diffractograms of zeolite 13X used as standard material and of the Fe-functionalized materials.

The comparison of the 13X matrix diffractogram with the infiltrated samples showed no significant changes in the material structure evidenced by the absence of secondary phases or loss of crystallinity (peaks intensity). This data indicates that the water-free infiltration procedure did not degrade the samples' structure.

As mentioned above, after the material preparation and prior to the methanation run the Fe-functionalized zeolite pellets need an activation step which is called reduction, consisting of the reduction of the oxidized Fe into metallic Fe, which is the active phase for methanation, by using heat combined with hydrogen (H_2).

This step is crucial to guarantee a well-performing material and parameters such as reduction temperature can rule its performance. A low temperature could not be sufficient to activate the material which would result in a lack of performance, as well as high temperatures, can lead to structural damage or complete destruction.

To probe the oxidation state of the Fe species in the catalysts and determine an optimal reduction temperature, temperature-programmed reduction experiments were performed, and the results are shown in Figure 14:

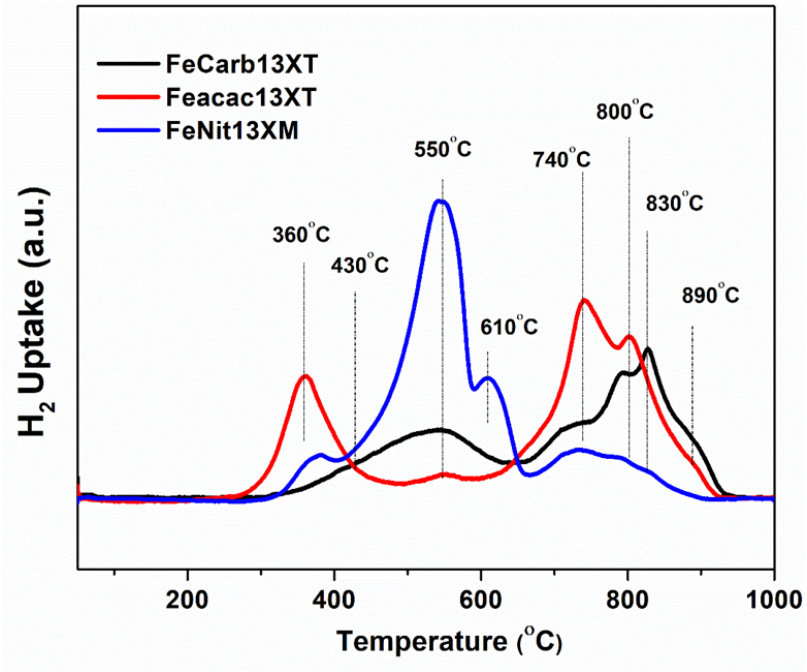

Figure 14 - Temperature programmed reduction profiles of the Fe-functionalized samples.

For the Feacac13XT (red) and Fenit13XM (blue), the reduction of Fe (III) to Fe (II) species can be observed at temperatures lower than 500ºC. The peak at 360ºC and the shoulder at ca. 430º C can be attributed to the reduction of zeolite extra framework Fe_2O_3 particles. Interestingly, for the Fecarb13XT, no defined peaks at temperatures lower than 500°C were observed. This can be related to the use of the iron(0)pentacarbonyl precursor, which seems not to undergo Fe species at the zeolite with high oxidation states, being limited to Fe(II) species which reduce at higher temperatures.

At temperatures between 500 to about 600°C for all samples, an H_2 uptake is observed, related to the reduction of Fe(II) species to metallic Fe. Peaks at temperatures above 600°C can be related to the reduction of Fe(II) to Fe metallic occurring in parallel with zeolite structure collapse (Li et al. 2008).

As observed in Figure 14, temperatures from 300 to 550°C may be required to activate the material, additionally, the knowledge acquired on SmartHiFe^2 indicates that 400°C is a good compromise between material activation and structure preservation, therefore this temperature will be used from now on.

The prepared materials were then submitted to a methanation run and the product distribution versus time is shown in Figure 15. The optimal parameters (reaction temperature = 400°C, pressure = 15 bar) used on the catalytic testing are the established ones according to the results obtained with the first generation of materials (Section 4.1).

In a typical methanation run, the high-pressure tubular reactor (d = 3 cm, L = 50 cm) was filled with about 180 g of catalyst, activated in H_2 flow, and followed by an inert gas purge a reactive mixture of H_2 and CO_2 (ratio 4.05) with a GHSV of 100 h^{-1} was passed through the reactor and the analysis of the resulting products was made on real-time with a mass spectrometer and the results for gas composition versus time are presented in Figure 15. The reactor was operated isothermally.

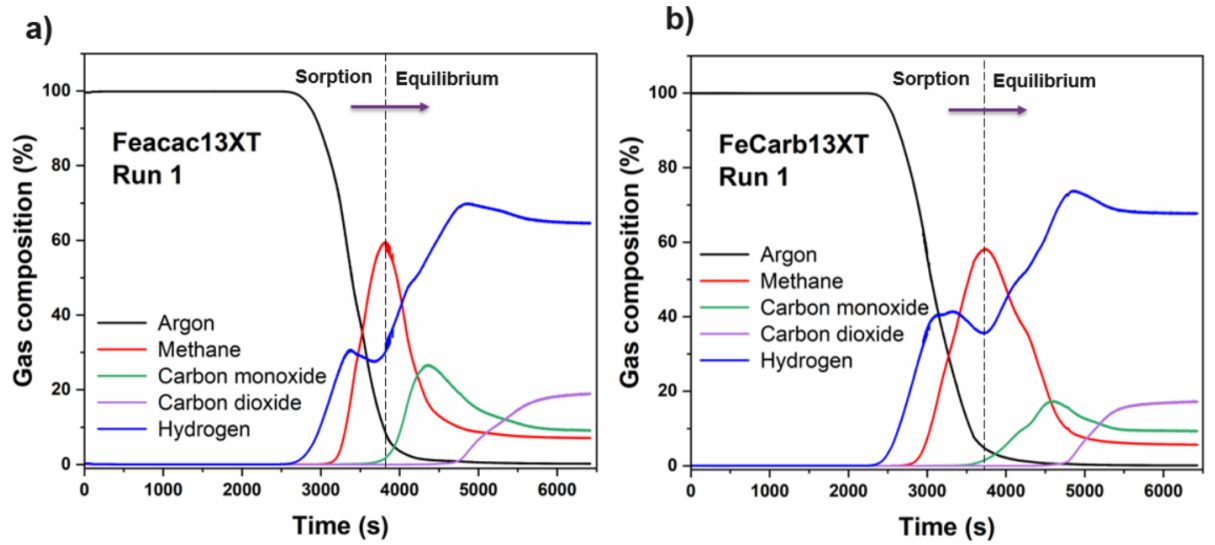

Figure 15 - Gas composition evolution vs time during methanation run with Fe-Zeolite materials. Conditions: T=400°C, pressure= 15 bar, and a GHSV of 100 h^{-1}.

As depicted in Figure 15, a clear separation between two zones of product distribution can be made, the sorption zone and the equilibrium zone. In the sorption zone, the zeolite acts as an adsorber, and the water formed during the reaction it is not released leaving the outlet stream composed mainly of CH_4. As the adsorption capacity is reached, the reaction enters the equilibrium zone, where the thermodynamic equilibrium is achieved, and the product distribution completely changes with the formation of carbon monoxide (CO) and CO_2 conversion decrease. In this state, the material behaves as a conventional catalyst, therefore, just the sorption mode zones will be considered. From the data in Fig.15, it was calculated the values of 99% CH_4 selectivity and 100% CO_2 conversion in sorption mode for both samples. This result indicates that the samples are active for methanation, and the water-free infiltration procedure was successful. Additionally, it is possible to correlate that even though the H_2-TPR results indicate that the Feacac13XT and Fecarb13XT have structurally distinguished Fe species, both were active for methanation, indicating that the Fe oxidation state of the active species was more relevant than the species structure. For instance, oligonuclear Fe species could be active as well as mononuclear Fe.

As important as the material synthesis and activity in the methanation reaction, stability and cyclability are crucial for the technology implementation. The ideal material should pull through hours of operation as well as several drying and/or reactivation cycles. In this regard, the samples were subjected to several methanation runs, and the product distribution results versus time are shown in Figure 16:

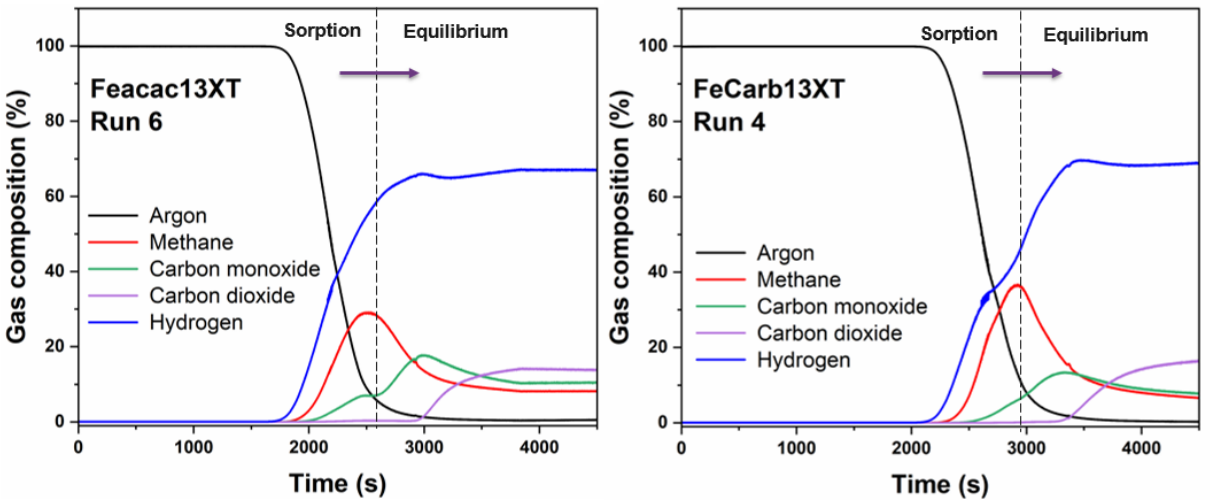

Figure 16 - Gas composition evolution vs time during methanation run with Fe-Zeolite materials. Conditions: T=400°C / Pressure= 15 bar / GHSV~ 100 h^{-1}.

To better visualize the material's behaviour during multiple methanation cycles, the results for CH_4 selectivity per methanation run (sorption zone) are shown in Figure 17. Comparing the methanation results for the first run and after several runs, it is clear, that the materials have decreased performance throughout the methanation cycles. Even though the sorption effect is still present, and the CO_2 conversion reached 100% in the sorption zone, a decrease in CH_4 selectivity is observed, evidenced by the formation of expressive amounts of CO.

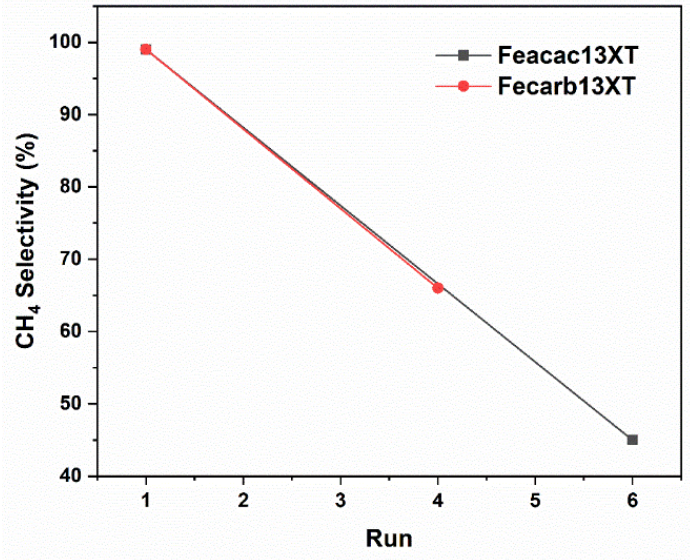

Figure 17 - CH_4 selectivity per methanation reaction run for the Fe-zeolite samples.

As observed in Fig. 17 the CH_4 selectivity decreased from 99% for both samples to 45% and 66% for the Feacac13XT and Fecarb13XT respectively. The conversion, on the other hand, remained the same (about 100%). This result suggests that the Fe species which were highly selective to CH_4 in the first run, are no longer selective, and they may be suffering from structure modification throughout the

reaction cycles due to dealumination or carbon accumulation, which is an undesired effect observed in metal-functionalized zeolites.
To identify the cause of decreased CH_4 selectivity, XRD measurements were performed in the samples after several reaction runs, and the results are shown in Figure 18:

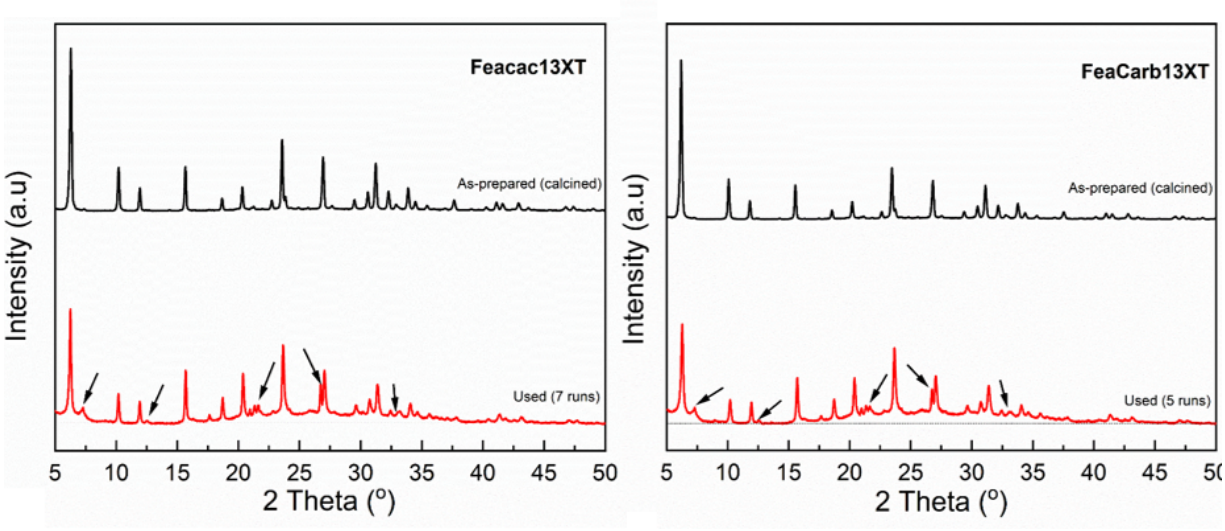

Figure 18 - XRD patterns for the Fe-Zeolites before and after the methanation reaction.

Structural changes can be observed by comparing the diffractograms collected before (as-prepared) and after (used) reactions. New peaks appeared, pointed out in Figure 18 by the black arrows, which may indicate a presence of an additional phase or a segregated phase of Fe oxide. Identifying the new phases is challenging since the diffraction pattern from the sample overlaps within the Fe phases. However, it is well known from the literature that bulk Fe-oxides in Fe-supported catalysts tend to be converted into Fe-carbides when submitted to certain conditions such as high temperatures/pressures in the presence of H_2 and CO (Figure 19) (Wezendonk et al. 2018).

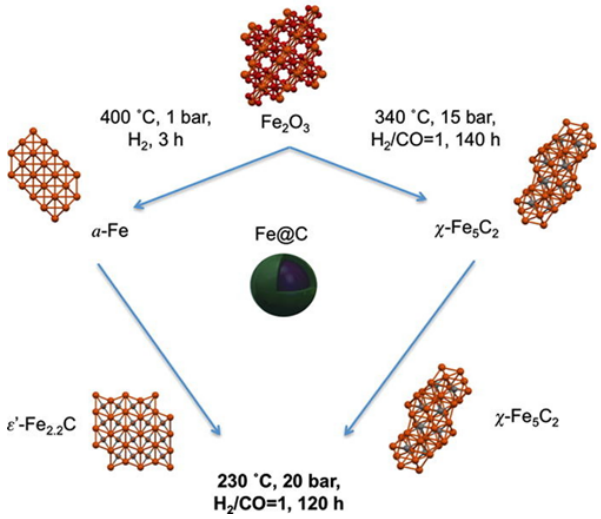

Figure 19 - Mechanisms for Fe-carbide formation from Fe_2O_3. Source: (Wezendonk et al. 2018).

The methanation reaction mechanism (Equations 1 and 2) is a combination of the reverse water-gas shift reaction and CO methanation (Baraj et al., 2016).

$$CO_2 + H_2 \leftrightarrow CO_{ad} + H_2O \quad \Delta H_{298K} = 41\ kJmol^{-1} \tag{1}$$

$$CO_{ad} + 3H_2 \leftrightarrow CH_4 + H_2O \quad \Delta H_{298K} = -206\ kJmol^{-1} \tag{2}$$

This means that CO is the main intermediate product, leading to carbide formation from the heat in combination with H_2 and CO-rich environment as is seen in Fig. 19. Decomposition of the formed Fe-carbides can be challenging depending on their type. Some carbides such as θ-Fe_3C may start to decompose at high temperatures ($>$ 500°C) and under vacuum treatment. It is possible that the carbide oxidated shell is retarding the decomposition of the θ-Fe3C core to α-Fe and C. These layers can be about 5 nm in thickness if any O species are available, which is valid in our application since the methanation reaction (reaction 1) leads to adsorbed CO which decomposes in C + O (Abel et al., 2019; Paalanen & Weckhuysen, 2020).

4.3 Increased performance by impeding metal deactivation

This section includes investigating the Fe-catalysts' performance in terms of loss activity by deactivation. As described above the materials have suffered from deactivation due to carbide formation. It is known that the best catalyst should balance the binding strength with the atoms and molecules: too weak bonding could not be enough to activate the reactants and too strong bonding could result in product decomposition instead of desorption, and this optimum bond strength is described by the 'Sabatier's principle' (Figure 20):

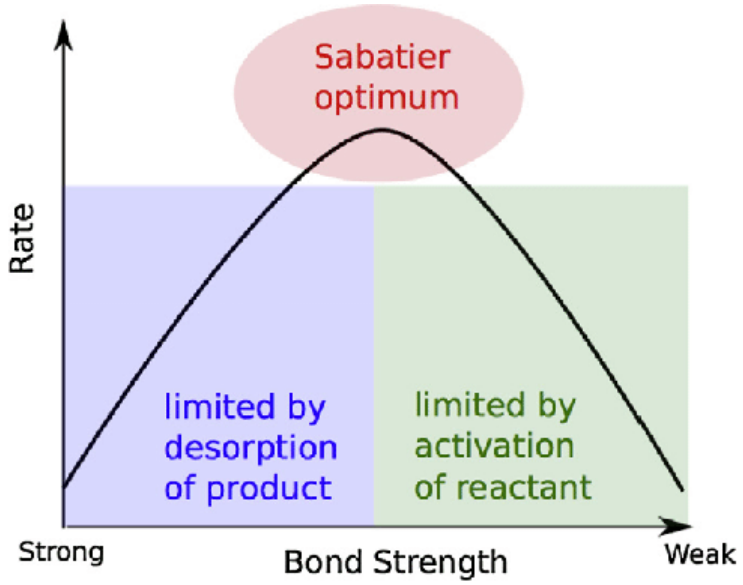

Figure 20 - Schematic representation of the 'Sabatier Principle'. Source:(Medford et al., 2015).

One of the strategies to impede metal deactivation by shifting the bond strength with the adsorbate is to dope the catalyst with another metal with "properties of interest". A fundamental understanding of the methanation reaction mechanism is important to pick the best candidate for doping, bringing the material

as close as possible to the 'Sabatier optimum'. Based on this knowledge, we chose three cost-extensive, non-noble metals for doping of the Fe-catalysts: zinc (Zn), nickel (Ni), and cobalt (Co).
Originally, in this project, it was proposed to dope Fe materials with Ni and Ru. New findings during the project allowed us to use non-noble metals instead of the expensive noble metal Ru with no performance prejudice. This approach is economically more advantageous and therefore it will be pursued from now on. The suitable synthesis route for doping with the chosen metals consists of a modification of the first-developed water-free Fe infiltration. The doping procedure consisted of a first infiltration with the doping metal (Zn, Ni, or Co) followed by the Fe infiltration using Fe(II)acetylacetonate, the used doping precursors, sample composition, and nomenclature are described in Table 6:

Table 6 - Metal precursors, metal weight content, and samples nomenclature.

Doping Precursor	Doping content (wt%)	Fe content (wt%)	Nomenclature
Zn acetate dihydrate	0.25	0.75	ZnFe13X
Nickel (II) nitrate hexahydrate	0.25	0.75	NiFe13X
Cobalt (II) nitrate hexahydrate	0.25	0.75	CoFe13X

After each infiltration, the material was dried at 120°C in a muffle and calcined in static air at 500° for 12 h.

4.3.1 ZnFe material

Following the Sabatier principle (Fig.20), Zn was chosen as a doping agent to further increase the carbon oxidation rate and suppress the Fe-carbide formation. The prepared ZnFe13X material then was submitted to methanation runs and the product distribution versus time is shown in Figure 21:

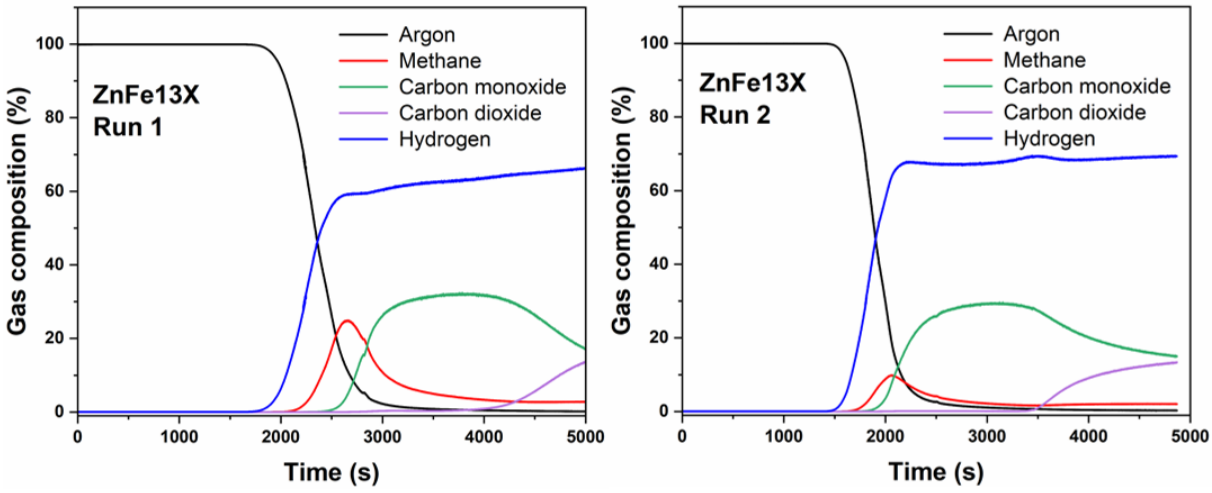

Figure 21 - Gas composition evolution vs time during methanation run with ZnFe13X sample. Conditions: T=400°C, pressure = 15 bar and GHSV = 100 h^{-1}.

The increased carbon oxidation effect by Zn doping was observed, evidenced by the expressive formation of CO. Consequently, there was a drop in the CH_4 formation and even though the CO_2 reached 99%, the CH_4 selectivity barely reached 40% in the first run. This effect was even more pronounced in the second run, with the CH_4 selectivity dropping to 17%. The conversion of CO_2 to CH_4 through the methanation reaction (Figure 22) occurs through adsorbed CO intermediate, and as important as the carbon oxidation is to avoid coking another aspect of the mechanism is crucial: the H_2 activation.

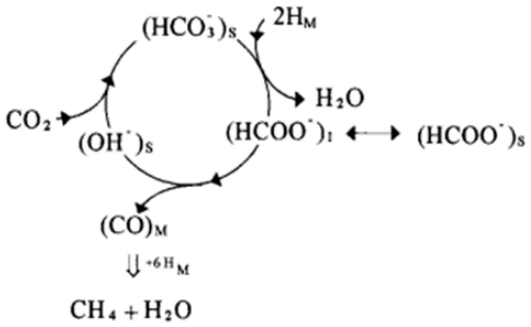

Figure 22 - First mechanism proposed for CO_2 methanation reaction. Source: (Baraj et al. 2016).

As described in Fig. 22, H_2 activation is crucial since to hydrogenate one molecule of adsorbed CO to CH_4, six atoms of adsorbed H atoms are required. These reactions, CO_2 adsorption, and H_2 activation take place simultaneously at the metal surface, and the bonding strength with the adsorbates again plays an important role. When we doped the Fe-materials with Zn, we may avoid the carbon deposition by increasing the carbon oxidation rate, but this will cost a decrease in the H_2 activation rate, affecting the CH_4 productivity. Therefore, Zn-doped materials were skipped.

4.3.2 NiFe material

Small amounts of Ni were incorporated into the Fe-materials with the intent to enhance the catalytic activity and selectivity towards CH_4 and the results of gas composition versus time are shown in Figure 23:

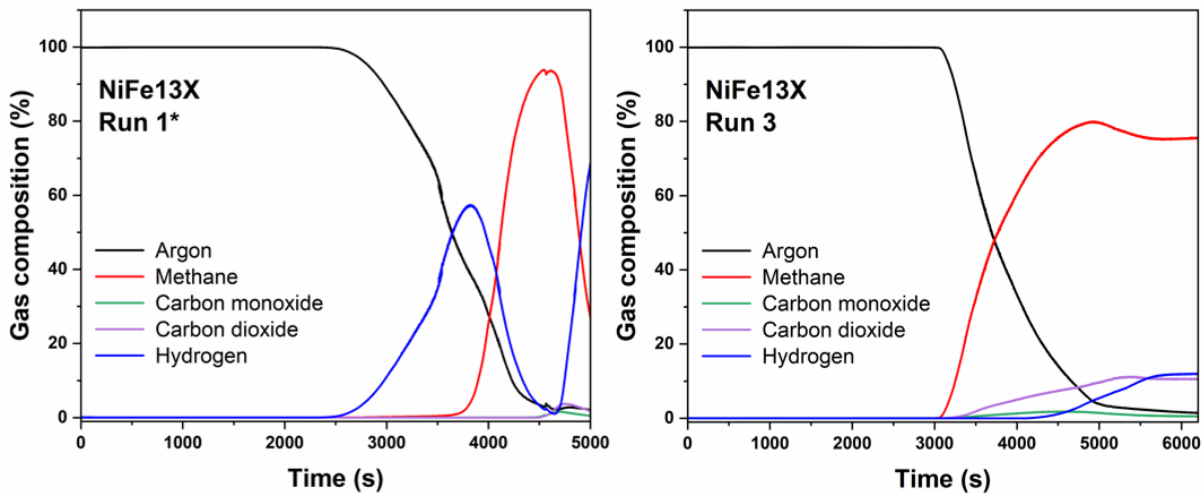

Figure 23 - Gas composition evolution vs time during methanation run with the NiFe13X sample. Conditions: T=400°C, pressure = 15 bar and GHSV = 100 h^{-1}.

For the Ni-doped sample, the CO_2 conversion and CH_4 selectivity reached 100 % in the first run. This result was expected since Ni is well known for its hydrogenation properties, however, the conversion dropped significantly in the third run, decreasing from 100% to 72%, and small amounts of CO were also observed, indicating material deactivation. XRD was performed after the methanation runs (Figure 24) and the diffractogram showed a loss of crystallinity when compared to the as-prepared sample data indicating possible structure collapse, which could explain the poor performance throughout the methanation runs.
Further investigation needs to be carried out to determine other causes of the deactivation, but we can assume that the zeolite structure collapsed, therefore pore blocking is caused, and loss of active surface area is significantly affecting the CO_2 conversion, even though the sorption effect was still observed.

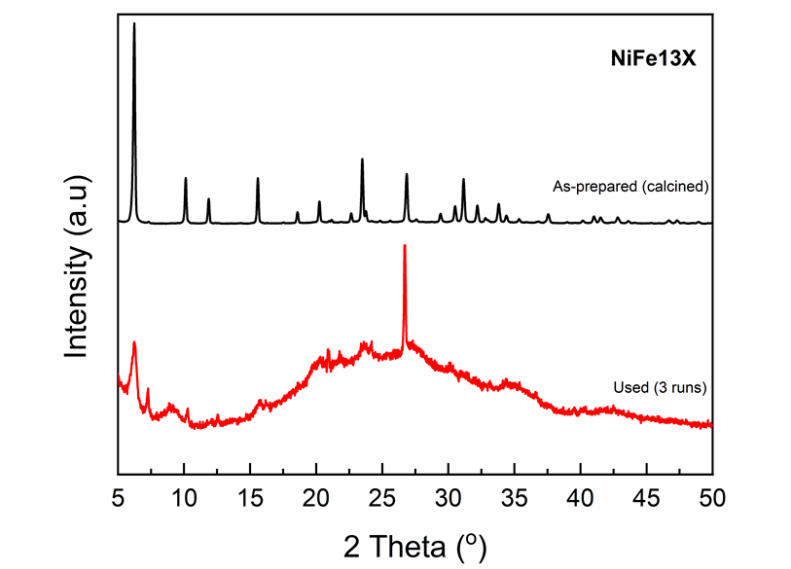

Figure 24 - XRD patterns of the NiFe13X sample, before (as-prepared) and after (used) methanation runs.

4.3.3 CoFe material

Lastly, the CoFe material, CoFe13X, was tested and the results of gas composition versus time during a methanation run are shown in Figure 25.

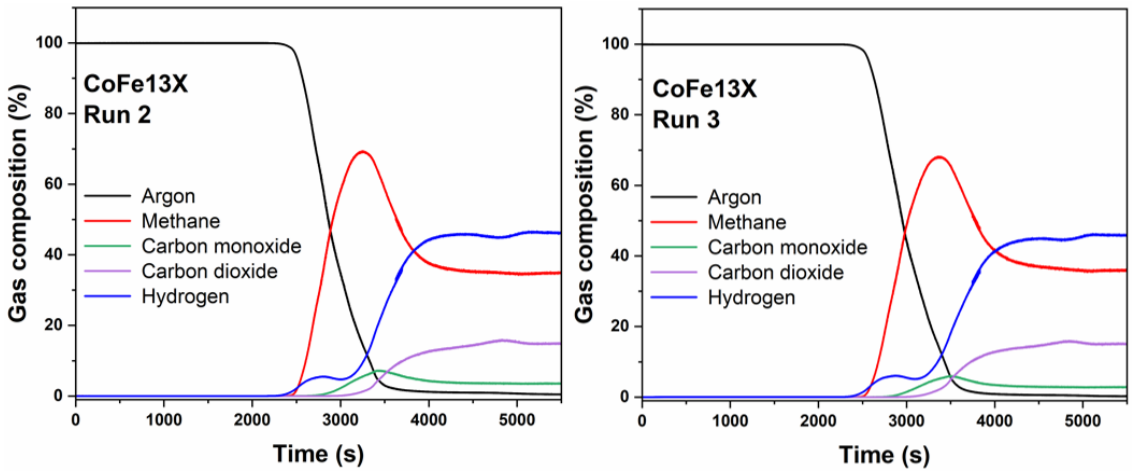

Figure 25 - Gas composition evolution vs time during methanation run with the CoFe13X sample. Conditions: T=400°C, pressure = 15 bar and GHSV = 100 h^{-1}.

The conversion reached 96% in the second run and the CH_4 selectivity was 94%. In the third run, both CO_2 conversion and CH_4 selectivity remained practically the same, indicating the sample's high stability. Even the product desorption, described by the shape of the curves, remained unchanged which is another indication of the high stability of this sample. According to the literature, the presence of Co-CoO sites promotes the oxidation of C* species and decreases carbon accumulation, consequently the formation of the carbide (Mizuno et al., 2017). As for the XRD results after the reaction (Figure 26), the diffractogram of the CoFe13X suggested that there was a loss of crystallinity, indicated by the decrease in peak intensity.

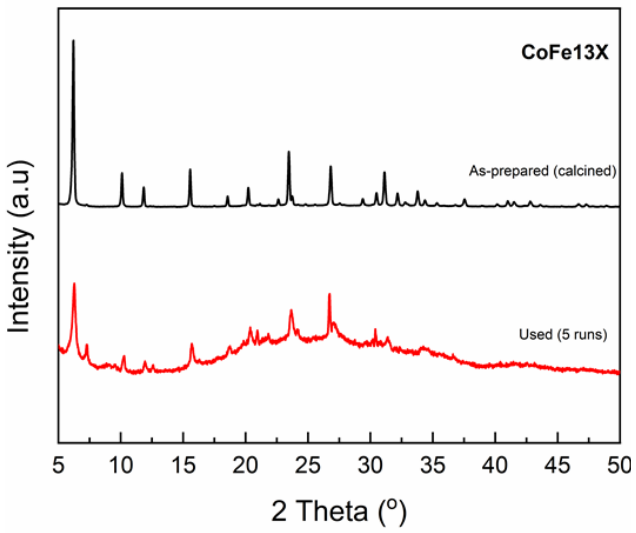

Figure 26 - XRD patterns of the CoFe13X sample, before (as-prepared) and after (used) methanation runs.

Even though a structural change was observed, the catalytic performance and the water adsorption capacity remained, since no loss in CO_2 conversion and CH_4 selectivity was observed (Fig. 25).
Among all the new Fe materials developed in this project, it is clear, that the Co-doped material presented the best performance not just in terms of CO_2 conversion and CH_4 selectivity but also in terms of stability. Hence, the CoFe13X material was chosen to fulfil the next steps of the project and to assure that the optimal reduction temperature was kept the same after the doping with cobalt, the oxidation state of the Co and Fe species in the catalysts was probed by temperature programmed reduction and the results are shown in Figure 27.
When compared to the monometallic Fe samples, it can be observed an average decrease of the reduction temperatures, with the first significant H_2 uptake at about 200°C which is probably related to extra framework oxide with the reduction from the species of Co(III) to Co(II) and Fe(III) to Fe(II). A further reduction to the Co(II) and Fe(II) occurs in temperatures in the range of 300°C to 500°C. Above 500°C the uptake is related to the reduction to a metallic state occurring in parallel with the zeolite structure collapse. The slightly lower reduction temperatures of the CoFe13X catalyst, when compared to the monometallic catalyst Feacac13XT, could be related to the formation of extra framework Fe and Co oxide species on the zeolite, which were more accessible than those in the zeolite inner structure. Thus, since no significant changes in the TPR were observed the optimal parameters determined in the previous section will be maintained.

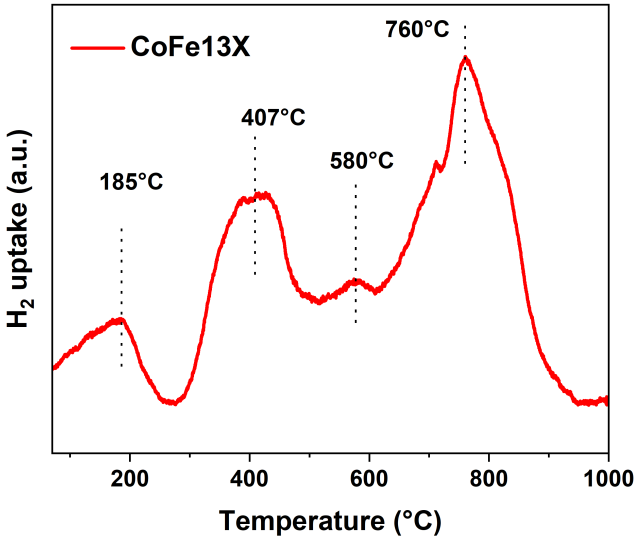

Figure 27 - Temperature programmed reduction profile of the CoFe13X sample.

4.4 Stability & degradation during sorption-enhanced methanation

When it comes to industrial application, additionally to high activity and selectivity, long-term stability is the most critical property of a catalyst (Hess et al., 2020; Schlögl, 2015). Therefore, material stability tests were performed as planned for WP3 using the CoFe13X material for 10 complete reaction cycles involving:

1. activation (H_2 reduction)
2. methanation reaction
3. regeneration by drying.

The results for CO_2 conversion and CH_4 selectivity per reaction run are presented in Figure 28:

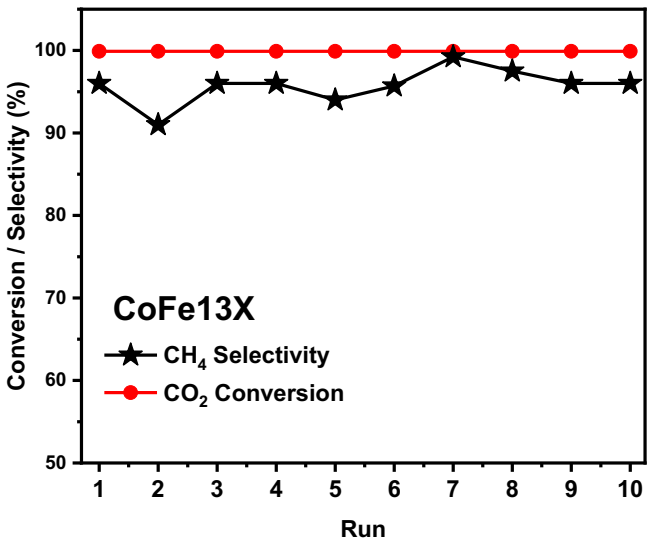

Figure 28 – CO_2 conversion and CH_4 selectivity per methanation reaction run using the CoFe13X material. Conditions: T=400°C, pressure = 15 bar and GHSV = 100 h^{-1}.

It can be observed that the CO_2 conversion was maintained over the 10 reaction runs and it was over 99%. As for the CH_4 selectivity, it fluctuated from 96 to 99% with an average of 97%. These results strongly indicate that the Co-doped material is not prone to deactivation by carbide phase formation. On the other hand, during methanation reaction is common that carbon deposits are formed over the catalyst causing deactivation. To investigate the carbon deposits formation Thermogravimetric Analysis was performed in the monometallic catalyst Feacac13XT and the Co-doped material, CoFe13X under two conditions:

1) In Nitrogen (N_2) atmosphere (Figure 29): this technique is used to identify the material weight lost due to adsorbed water. Usually, the mass loss associated with physisorbed water occurs in the range of 30-250°C (Li et. al., 2001)
2) In Oxygen (O_2) atmosphere (Figure 30): this technique is used to identify the material weight lost due to oxidizable carbon deposits. Mass losses associated with carbon deposits are identified in temperatures over 300°C (Mizuno et al., 2017)

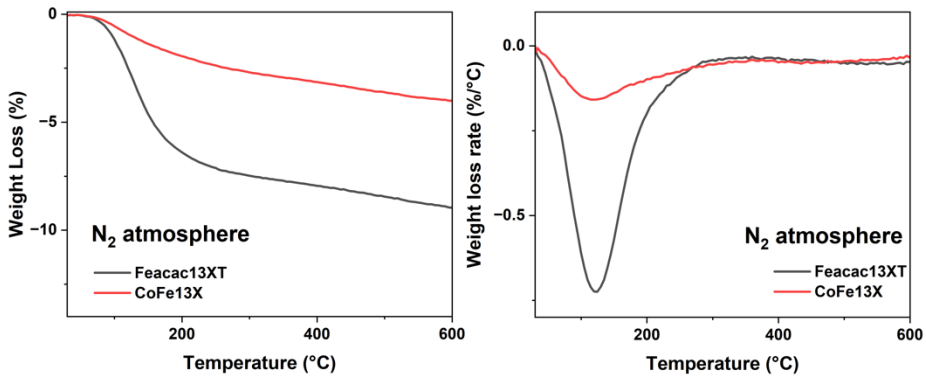

Figure 29 - TGA results under N_2 atmosphere for the Feacac13XT and CoFe13X.

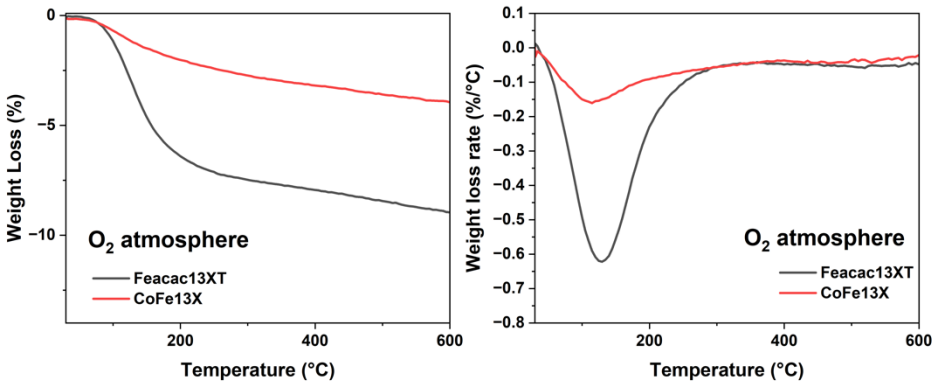

Figure 30 - TGA results under O_2 atmosphere for the Feacac13XT and CoFe13X.

In Figure 29 and Figure 30, it can be observed one region of weight loss in the temperature range of 30-200°C related to the release of water molecules adsorbed in the zeolite (Li et al., 2001; Ramli & Amin, 2015). Interestingly, the change of the atmosphere from N_2 (Figure 29) and O_2 (Figure 30) seems not to affect the weight loss for both samples. It can be assumed that there was no carbon deposit formation over the Co-doped material since just weight loss at low temperatures was identified even under an oxidative atmosphere and it is only related to adsorbed water.

While for the monometallic catalyst Feacac13X, it is plausible that the carbon is converted to a persistent Fe-Carbide phase, as evidenced by the XRD results (Fig.18) and, this phase is persistent and not easily decomposed even under an oxidative atmosphere as mentioned previously (Figure 19), which also explains why there was no weight loss related to carbonaceous species.

4.5 Continuous high-quality CH_4 production using an automated twin-reactor system

In order to achieve the maturity of the sorption-enhanced technology, enable an effective continuous operation by optimizing the regeneration (drying) time was investigated using the already established nickel-based material (Delmelle et al., 2016).
The principle of sorption-enhanced methanation is the zeolite acting as an adsorber for the water produced during the methanation reaction shifting the equilibrium to the product side leading to a 100% CH_4 yield. However, when the zeolite reaches its adsorption capacity, removal of the adsorbed water is needed, a regenerative step is then started and during this time no methanation can be performed (Delmelle et al., 2016, 2018). To overcome this challenge, a “twin-reactor system” (Figure 31) was developed to ensure continuous CH_4 production by alternating the reactors between CH_4 production and regeneration.

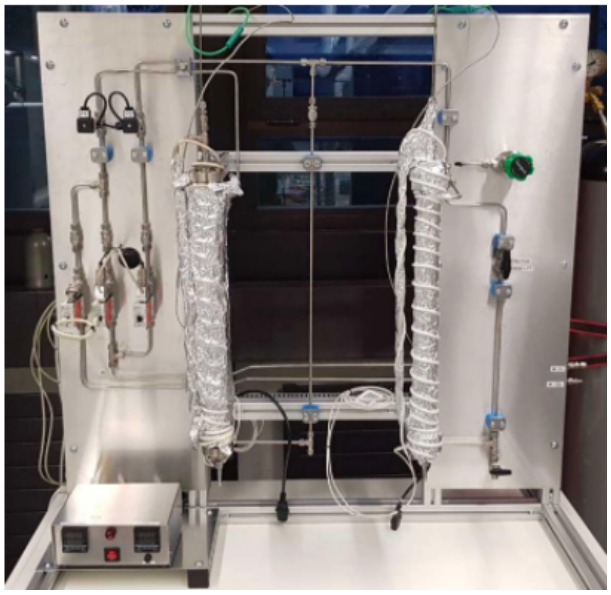

Figure 31 - Automated twin-reactor system equipped with MEMs sensors.

To guarantee the feasibility of this technology for industrial applications, automation of the twin-reactor system was made using MEMs sensors. The automation allows the automatic reactor switch when the sensor identifies a drop in the gas quality, which is equivalent to the reaching of the material water adsorption capacity. To achieve the 1/1 ratio between CH_4 production and regeneration time an adjustment in the gas hourly space velocity (GHSV) needed to be made. The methanation reaction was carried out at ambient pressure, 300°C, and a GHSV = 60 h^{-1}. The regeneration step (drying) was carried out at the same temperature and pressure but with a GHSV = 571 h^{-1}. Methane was used as a drying gas. The results of gas composition per time using the twin-reactor system during a typical methanation run are presented in Figure 32:

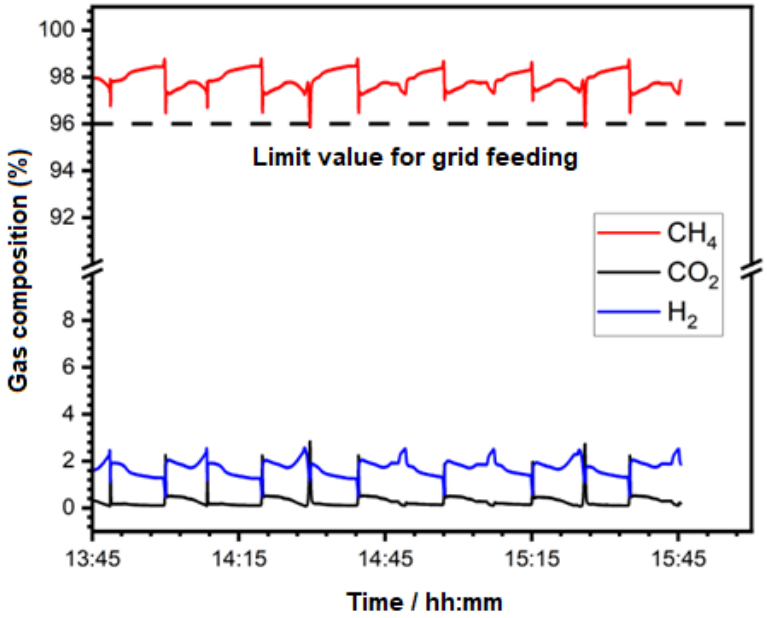

Figure 32 - Gas composition vs time for a typical methanation run in the twin-reactor system obtained by mass spectroscopy. Conditions: Conditions: T=300°C, pressure = 1 bar, GHSV = 60 h^{-1} (methanation) and GHSV = 571 h^{-1} (regeneration).

As observed in Figure 32, the twin-reactor system was operated automatically for 12 consecutive cycles (over 2 hours) and gas quality was an average of 98% dry CH_4 which could be easily injected into the gas grid without any post-treatment. The robustness of the automatic sensor switch was also proved to be successful.

4.6 Proof of concept of SmartHiFe^2 system in the research platform HEPP

As mentioned in Section 3.1, a 10 L reactor was provided by our partner Fluitec Switzerland, which brings us closer to a real industrial scenario. This reactor is part of the proof-of-concept in SmartHiFe^2 through its implementation in the research platform at OST. As the first step for implementation, the reactor was operated in our lab facility connected to scientific equipment for better process analysis, to extract the optimum operational parameters and test the system reliability.
Strategically, we opted to work with the already established nickel-based system (Delmelle et al., 2016) since the operational parameters (temperature, GHSV, pressure) were already defined for the Lab scale, and therefore the obtained data was easier to analyse. The first tests with the Fluitec reactor were performed in our lab facilities and the results of gas composition versus time were therefore obtained for the Ni13X sample during a methanation run (Figure 33):

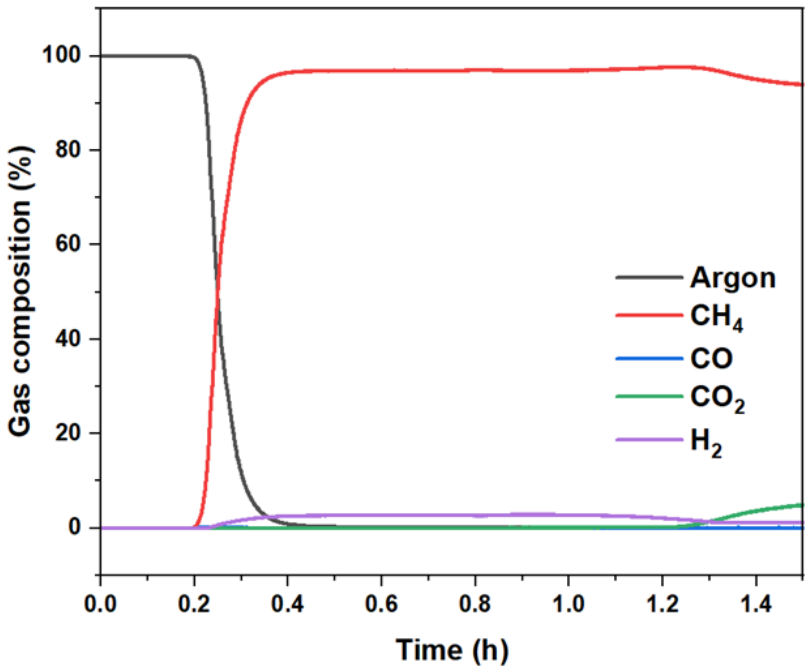

Figure 33 - Gas composition evolution vs time during methanation run with the Ni13X sample. Conditions: T=300°C, pressure = 1 bar and GHSV = 100 h^{-1}.

In the sorption zone, the gas composition reached 97% CH_4 with a CO_2 conversion of 100%. It must be mentioned that due to a mass flow controller calibration problem, the used inlet gas ratio of H_2 / CO_2 = 3.8 was not at the optimal ratio of H_2 / CO_2 = 4.0, a fact that affected the CH_4 production since previous results for the nickel-based system described a product stream composed by 100% CH_4 in sorption mode. Even at this condition, the system was extremely stable, and the expected results for the first test were achieved, 97% of the out-stream gas was composed of CH_4 and just the sorption mode time was shortened. This is encouraging since all the knowledge obtained with the nickel-based system for such a large system can now be transferred to SmartHiFe^2 bringing us a step closer to its implementation.

5 Conclusions

At the beginning of the funding period, functionalization with Fe was carried out not only on the finished pellet but also on zeolite powder, the so-called “first generation of Fe-zeolite materials”. In the further course, the activity of the catalysts about CO_2 methanation could also be tested. Unfortunately, preliminary tests showed that despite variable initial conditions (activation, temperature, flow), the Fe(II)-sulfate-based system did not yield any methane. This is attributed to the sulfur presence even after prolonged calcination, which poisoned the catalytic centres. On the other hand, self-prepared pellets (>140 g) functionalized with Fe(III)-nitrate and Fe(II)-chloride showed both activity in CO_2 methanation and the presence of a sorption effect under different reaction conditions (T = 350 - 450°C, p = 0 - 21 bar). The best values with selectivity up to 92% at T = 400°C and p = 15 bar were shown by the Fe(II)-Chloride material. However, the conversion did not exceed 90 %.
Progress was also made regarding the composition of the pellets; in addition to a protocol for templating, a protocol for the selective etching of the zeolite structure was also established. Regarding existing degradations, initial efforts were made to understand the underlying mechanisms. It is assumed that too high activation/reaction temperatures can lead to degradation of the pore system. Regarding the oxidation sensitivity of the catalyst, it was found that subsequent activation fully restores the functionality.

The establishment of a water-free infiltration method allows us now to aim for even cheaper well-performing materials, the so-called “second generation”. There is a strong relationship between the Fe precursor used in the synthesis and the Fe species formed into the zeolite, however, the activity for methanation seems to be related to the Fe species oxidation state, not to its structure. This is an unexpected but important finding for the SmartHiFe^2 technology.
Even though it was possible to produce structurally different Fe-functionalized materials by varying the precursors, all Fe-materials present deactivation with the methanation cycles losing an average of 50% CH_4 selectivity throughout the cycles. This deactivation seems to be related to Fe-carbide phase formation. This new phase is resistant to carburization, and avoiding its formation is the only reasonable solution to prevent catalyst deactivation.
Impeding the deactivation by metal doping was a successful approach. For economic reasons, we chose non-noble metals for this task: Zn, Ni, and Co. A suitable synthesis route for metal doping was successfully defined on the base of a water-free Fe infiltration procedure.
Although the doping with Zn and Ni was successful in terms of synthesis, the materials presented inferior performance towards methanation. For the Zn-doped material, an excessive overoxidation of the adsorbed carbons led to an increase in CO formation rate instead of CH_4. Additionally, the H_2 activation was not enough to provide the adsorbed H atoms necessary to complete the methanation reaction, which again led to CO desorption. As for the Ni-doped materials, remarkable results for CO_2 conversion and CH_4 selectivity were obtained (~100% for both) in the first reaction cycle, however, when submitted to multiple reaction cycles, the material collapsed, which was evidenced by the XRD results, lacking in performance with a huge drop in the conversion.
Lastly, the Co-doped material had the best performance in terms of CH_4 selectivity (~97%), CO_2 conversion (≥99%), and stability toward cycling, with the performance maintained for ten consecutive cycles. TGA results also supported the assumption of the coke resistance of the Co-Fe material, no weight losses related to carbonaceous deposits were identified.
Progress was also made in terms of SEM technology maturity. By developing a twin-reactor reaction system operating with the already established nickel material for sorption-enhanced technology, a quasi-continuous high-quality CH_4 (98%) production with no moisture was achieved, with the advantage of the plant being fulling automated. At the end of the funding period, it was clear that the SmartHiFe^2 concept can be a successful approach with the newly developed materials, which are less impactful to the environment.

6 Outlook and next steps

The findings of this project helped to increase the maturity of the Sorption Enhanced Methanation Technology. From the scientific point of view, it is the first time that iron-based systems are reported as successfully active for the methanation reaction. Economic aspects were taken into consideration and a complete replacement of nickel by the cost-effective iron was achieved.
Despite the state of the SmartHiFe^2 technology being promising and closer to an implementation step, some open questions need to be addressed for a successful long-term operation in an industrial application. That would be related to the robustness of the SmartHiFe^2 system in a real site. A screening of implementation sites needs to be done to select the most suitable plant to implement SmartHiFe^2 technology on a pilot level. Aspects such as biogas composition and the presence of contaminations that could cause material deactivation (i.e. H_2S) need to be evaluated.
The establishment of the material lifetime is also an important parameter to be addressed. Hereby, it was demonstrated that the SmartHiFe^2 system can be operated with no loss of performance for 10 consecutive reaction cycles, however longer times of operation, at least 50 complete reaction cycles, and

that on automated routines (e.g. Labview or even industrially suitable SPS systems) are necessary to predict the material behaviour over usage.
In terms of an industrial proof-of-concept, it is highly desired to achieve continuous sorption-enhanced production of biomethane with a 1:1 ratio of methanation time to regeneration time. Results presented in this report demonstrated that is possible to continuously produce high-quality methane (~96% purity) for a nickel-based (SmartCat) system. But operation conditions for Fe-based materials differ quite a lot in temperature and pressure, resulting also in different adsorption-desorption behaviour, gas diffusion, and capillary effects. This must be investigated and demonstrated using the high-potential SmartHiFe^2 system before its successful industrialization.

7 National and international cooperation

The new laboratory “Advanced Materials and Processes” (AMP) was recently founded at the Institute of Environmental and Processing Technology (UMTEC, www.umtec.ch) at the newly established OST (Eastern Switzerland University of Applied Sciences), In this first phase, several national cooperation was established.

- A German consortium is willing to integrate SmartCat/SmartHiFe^2 technology in terms of the reuse of landfill-based CO_2. UMTEC is currently in negotiation.
- Strategic partnership with Micromeritics (Germany, manufacturer of analytic devices) for catalyst analysis
- Strategic partnership with Fluitec (Switzerland): Industrial reactor design, scale-up, and manufacturing
- MEMS AG (Switzerland), Sensor-based automation of twin reactors as industrial reactor module
- Edward Neibauer (CEO of Catalyst Midstream Companies) for integration of the sorption-enhanced system in the US plant.
- Clariant Produkte GmbH (Germany), Global Product Manager Fuel Upgrading Catalysts

8 Communication

- Aqua & Gas, No 11, 2023, 45-49: Darf Es Ein Wenig Mehr Sein? – Ein Hochleistungsreaktor für hohe Gasqualität und hohe Produktionsraten.
- Jahresbericht 2021 Gaz & Energie, Verband der Schweizerischen Gasindustrie: “Ringen um die richtige Klimapolitik”
- UMTEC Newsletter 1 (02/2020): Synfuels – From Lab to Industry
- 24. Erfahrungsaustausch PtX (ERFA), Limeco Dietikon, oral presentation: “A novel iron-based catalytic biogas upgrade concept”
- Bioenergieforschung in der Schweiz 2023, oral presentation: “Ein neuartiges katalytisches Biogasaufbereitungskonzept auf Eisenbasis–SmartHiFe^2”
- Energate Messenger, “Forscher steigern Biogasertrag um bis zu 30 Prozent”. Available online: https://www.energate-messenger.ch/news/232438/forscher-steigern-biogasertrag-um-bis-zu-30-prozent

- Aqua & Gas, “Ideen für mehr Biogas”. Available online: https://www.aquaetgas.ch/de/aktuell/branchen-news/20230511_ideen-für-mehr-biogas/
- EE News, Colloque “La recherche sur la bioénergie en Suisse”: Nouvelles idées pour plus de biogaz. Available online: https://www.ee-news.ch/de/article/51386/colloque-la-recherche-sur-la-bioenergie-en-suisse-nouvelles-idees-pour-plus-de-biogaz&page=#article_51386
- 14. Expertinnengespräche Power-to-X, oral presentation: “Neue Technologien zur Methanisierung im Projekt HEPP”.
- Further public communication activities via LinkedIn.

9 Publications

- Are Fe-based catalysts an upcoming alternative to Ni in CO_2 methanation at elevated pressure? Tanja Franken and Andre Heel, Journal of CO_2 Utilization, Volume 39, 101175, July 2020. DOI: 0.1016/j.jcou.2020.101175
- Additional publication in preparation.

10 References

Abel, F. M., Pourmiri, S., Basina, G., Tzitzios, V., Devlin, E., & Hadjipanayis, G. C. (2019). Iron carbide nanoplatelets: Colloidal synthesis and characterization. *Nanoscale Advances*, *1*(11), 4476–4480. https://doi.org/10.1039/c9na00526a

Baraj, E., Vagaský, S., Hlinčik, T., Ciahotný, K., & Tekáč, V. (2016). Reaction mechanisms of carbon dioxide methanation. In *Chemical Papers* (Vol. 70, Issue 4, pp. 395–403). De Gruyter Open Ltd. https://doi.org/10.1515/chempap-2015-0216

Borgschulte, A., Delmelle, R., Duarte, R. B., Heel, A., Boillat, P., & Lehmann, E. (2016a). Water distribution in a sorption-enhanced methanation reactor by time-resolved neutron imaging. *Physical Chemistry Chemical Physics*, *18*(26), 17217–17223. https://doi.org/10.1039/c5cp07686b

Delmelle, R., Duarte, R. B., Franken, T., Burnat, D., Holzer, L., Borgschulte, A., & Heel, A. (2016). Development of improved nickel catalysts for sorption-enhanced CO2 methanation. *International Journal of Hydrogen Energy*, *41*(44), 20185–20191. https://doi.org/10.1016/j.ijhydene.2016.09.045

Delmelle, R., Terreni, J., Remhof, A., Heel, A., Proost, J., & Borgschulte, A. (2018). Evolution of water diffusion in a sorption-enhanced methanation catalyst. *Catalysts*, *8*(9). https://doi.org/10.3390/catal8090341

El-Naggar, A., Ahmed, N., Mosa, A., Niazi, N. K., Yousaf, B., Sharma, A., Sarkar, B., Cai, Y., & Chang, S. X. (2021). Nickel in soil and water: Sources, biogeochemistry, and remediation using biochar. *Journal of Hazardous Materials*, *419*. https://doi.org/10.1016/j.jhazmat.2021.126421

Franken, T., & Heel, A. (2020). Are Fe-based catalysts an upcoming alternative to Ni in CO2 methanation at elevated pressure? *Journal of CO2 Utilization*, *39*. https://doi.org/10.1016/j.jcou.2020.101175

Hess, F., Smarsly, B. M., & Over, H. (2020). Catalytic Stability Studies Employing Dedicated Model Catalysts. *Accounts of Chemical Research*, *53*(2), 380–389. https://doi.org/10.1021/acs.accounts.9b00467

Li, Z., Xie, K., & Slade, R. C. T. (2001). Studies of the interaction between CuCl and HY zeolite for preparing heterogeneous Cu I catalyst. In *Applied Catalysis A: General* (Vol. 209).

Medford, A. J., Vojvodic, A., Hummelshøj, J. S., Voss, J., Abild-Pedersen, F., Studt, F., Bligaard, T., Nilsson, A., & Nørskov, J. K. (2015). From the Sabatier principle to a predictive theory of transition-metal heterogeneous catalysis. *Journal of Catalysis*, *328*, 36–42. https://doi.org/10.1016/j.jcat.2014.12.033

Mizuno, S. C. M., Braga, A. H., Hori, C. E., Santos, J. B. O., & Bueno, J. M. C. (2017). Steam reforming of acetic acid over MgAl2O4-supported Co and Ni catalysts: Effect of the composition of Ni/Co and reactants on reaction pathways. *Catalysis Today*, *296*, 144–153. https://doi.org/10.1016/j.cattod.2017.04.023

Paalanen, P. P., & Weckhuysen, B. M. (2020). Carbon Pathways, Sodium-Sulphur Promotion and Identification of Iron Carbides in Iron-based Fischer-Tropsch Synthesis. In *ChemCatChem* (Vol. 12, Issue 17, pp. 4202–4223). Wiley Blackwell. https://doi.org/10.1002/cctc.202000535

Pfaff, G. (2021). Iron oxide pigments. *Physical Sciences Reviews*, *6*, 535–548. https://doi.org/10.1515/b_psr-2020-0179

Ramli, N. A. S., & Amin, N. A. S. (2015). Fe/HY zeolite as an effective catalyst for levulinic acid production from glucose: Characterization and catalytic performance. *Applied Catalysis B: Environmental*, *163*, 487–498. https://doi.org/10.1016/j.apcatb.2014.08.031

Schlögl, R. (2015). Heterogeneous catalysis. In *Angewandte Chemie - International Edition* (Vol. 54, Issue 11, pp. 3465–3520). Wiley-VCH Verlag. https://doi.org/10.1002/anie.201410738

Shetti, V. N., Kim, J., Srivastava, R., Choi, M., & Ryoo, R. (2008). Assessment of the mesopore wall catalytic activities of MFI zeolite with mesoporous/microporous hierarchical structures. *Journal of Catalysis*, *254*(2), 296–303. https://doi.org/10.1016/j.jcat.2008.01.006

Terreni, J., Trottmann, M., Franken, T., Heel, A., & Borgschulte, A. (2019). Sorption-Enhanced Methanol Synthesis. *Energy Technology*, *7*(4). https://doi.org/10.1002/ente.201801093

Verboekend, D., Vilé, G., & Pérez-Ramírez, J. (2012). Hierarchical y and USY zeolites designed by post-synthetic strategies. *Advanced Functional Materials*, *22*(5), 916–928. https://doi.org/10.1002/adfm.201102411

Wezendonk, T. A., Sun, X., Dugulan, A. I., van Hoof, A. J. F., Hensen, E. J. M., Kapteijn, F., & Gascon, J. (2018). Controlled formation of iron carbides and their performance in Fischer-Tropsch synthesis. *Journal of Catalysis*, *362*, 106–117. https://doi.org/10.1016/j.jcat.2018.03.034

Xing, Y., Yan, B., Lu, P., Cui, X., Li, L., & Wang, M. (2017). Purification of Hg0 from flue gas by wet oxidation method and its mechanism: a review. In *Environmental Science and Pollution Research* (Vol. 24, Issue 34, pp. 26310–26323). Springer Verlag. https://doi.org/10.1007/s11356-017-0480-6

11 Appendix

No Appendix data.